



Early Oligocene dinocysts as a tool for palaeoenvironment reconstruction and stratigraphical framework – a case study from a North Sea well

Kasia K. Śliwińska

Stratigraphy Department, Geological Survey of Denmark and Greenland, GEUS,
Øster Voldgade 10, 1350 Copenhagen K, Denmark

Correspondence: Kasia K. Śliwińska (kksl@geus.dk)

Received: 26 June 2018 – Revised: 18 May 2019 – Accepted: 29 May 2019 – Published: 2 September 2019

Abstract. The lower Oligocene (Rupelian) successions are climate record archives of the early icehouse world in the Cenozoic. Even though the number of studies focussing on the generally cold Oligocene is increasing, little is known about climatic variations in the mid-latitudes to high latitudes of the Northern Hemisphere. One of the major obstacles is the lack of stratigraphically complete uppermost Eocene to Oligocene successions in these regions. This study focusses on dinoflagellate cysts (dinocysts) from a thick nearly complete Rupelian succession in the Syracuse Oils Norge A/S well 11/10-1 drilled in 1969 in the Norwegian part of the North Sea basin. The well provides a record of mid-latitude dinocyst assemblages, which yield key biostratigraphical and palaeoenvironmental information.

All the analyses were undertaken on ditch cutting samples. The dinocyst assemblages confirm that the well penetrates about 600 m of Rupelian sediments and (as supported by correlation with the Nini-1 well) that the lowermost Rupelian (below the top or the last occurrence of *Areosphaeridium diktyoplokum*) is expanded. These assemblages also indicate the presence of two hiatuses: the first extends from the Lutetian to the Priabonian (equivalent to the D9nb–D12nb zones), and the second spans the Rupelian–Chatian boundary (equivalent to the D14nb subzone or the NSO-5 zone). Despite the risk of caving, the dinocyst assemblages support the existing sequence stratigraphic framework. The assemblages reflect a clear transition from distal to proximal deposition in the vicinity of the site (across the regional seismic sequences OSS-1 – OSS meaning Oligocene seismic sequence – to OSS-2). The proximal deltaic deposits of the OSS-2 regressive system tract (RST) are characterised by pulses of high sea-surface productivity and pronounced shifts in the dinocyst assemblages, reflecting a highly dynamic environment in a restricted marine to marginal marine setting.

The Rupelian succession penetrated by well 11/10-1 yields one new species, *Areoligera? barskii* sp. nov., which is described here in detail.

The cold-water-tolerant dinocyst *Svalbardella cooksoniae* is present in two intervals in the studied succession. These intervals are related to the early Oligocene cooling maxima (the Oi-1a and the Oi-2 events). Furthermore, these two intervals correlate with two local sequence boundaries, suggesting that they are most probably of glacioeustatic origin. From these observations, I postulate that the early icehouse climate played an important role in the depositional development of the Oligocene succession in the North Sea basin. Even though the Eocene–Oligocene transition interval is not complete (i.e. Lutetian to Priabonian is either missing or condensed), well 11/10-1 merits high-resolution studies of the early icehouse climate for the North Sea region. Although any detailed studies should ideally be undertaken on conventional cores instead of ditch cuttings, no such samples spanning the Eocene–Oligocene transition exist in this area.

1 Introduction

The Rupelian (early Oligocene; 33.9–28.1 Ma; Vandenberghe et al., 2012) represents the first stage of the early icehouse world. Establishment of the permanent ice cap on Antarctica (e.g. Galeotti et al., 2016; Zachos et al., 1992) and the possible appearance of isolated continental glaciers on Greenland (e.g. Eldrett et al., 2007; Tripathi and Darby, 2018) had a global impact on ocean structure (e.g. Coxall et al., 2005) and flora and fauna (e.g. Sun et al., 2014). It also coincided with a shift from hemipelagic to siliciclastic sedimentation in many worldwide locations, including Antarctica (Bartek et al., 1991), Africa (Lavie et al., 2001), the western North Atlantic (Pekar et al., 2000) and the eastern North Sea basin (Michelsen et al., 1998). As shown by the deep-sea proxy record (e.g. Ocean Drilling Program sites 529 and 1218), there were several glaciation events during the Oligocene in Antarctica. These are known as Oi events (Pälike et al., 2006; Pekar and Miller, 1996). At deep-sea sites with a more continuous record, Oi events are expressed as positive excursions in the oxygen isotopic record of benthic foraminifera (Miller et al., 1991; Pälike et al., 2006; Wade and Pälike, 2004). In continental margin settings, these cooling events are often associated with hiatuses (Pekar et al., 2002; Pekar and Miller, 1996) linked to glacioeustatic sea-level falls. At least five of these cooling events, i.e. Oi-1 (earliest C13n), Oi-1a (early C12r), Oi-2 (C11r), Oi-2a (early C9r) and Oi-2b (middle C9n), took place during the Rupelian–earliest Chattian (Miller et al., 1998; Pälike et al., 2006; Wade and Pälike, 2004). Three of the Oligocene cooling maxima in the central North Sea basin (Oi-1a, Oi-2 and Oi-2b) correspond to the appearance of the cold-water dinocyst taxa *Svalbardella cooksoniae* and/or *Svalbardella* spp. (Clausen et al., 2012; Van Simaeyns et al., 2005a; Śliwińska et al., 2010; Śliwińska and Heilmann-Clausen, 2011).

The type section for the Rupelian stage is located in the southern North Sea basin (i.e. the Boom Clay Formation in NW Belgium; e.g. Abels et al., 2007; Lagrou et al., 2004; Van Simaeyns et al., 2004; Van Simaeyns and Vandenberghe, 2006), where the deposits consist primarily of mudstones (Schjøler et al., 2007; Van Simaeyns and Vandenberghe, 2006). Even though the Rupelian succession is more complete in the stratotype area than onshore in Denmark, the cumulative thickness of the Rupelian clays in both areas does not exceed 150 m (see Van Simaeyns et al., 2004; Śliwińska et al., 2012). In contrast, in the Danish and Norwegian sectors of the North Sea basin (i.e. NE North Sea basin), the siliciclastic clinoforms of Oligocene age are up to 1000 m thick and seem to represent a more complete record than onshore (Clausen et al., 2012; Michelsen et al., 1998; Śliwińska et al., 2010).

However, currently there is not a single sediment core in the NE North Sea basin that penetrates Oligocene strata. With the exception of few side-wall core samples from a single well in the central North Sea basin (Van Simaeyns, 2004), all the sediments available for analysis are ditch cut-

tings from industrial wells. Such samples cannot be used for magnetostratigraphic and organic proxy analyses (Śliwińska et al., 2014b) and limit the study of organisms to microfossils (e.g. foraminifera, calcareous nannofossils and dinocysts). Moreover, planktic foraminifera and calcareous nannofossil assemblages are very impoverished in the Oligocene deposits in the NE North Sea basin (e.g. King et al., 2016; Śliwińska et al., 2012) in relation to the Tethys (Coccioni et al., 2018; Śliwińska et al., 2014a, b) or the eastern North Atlantic (e.g. de Kaenel and Villa, 1996; Snyder and Waters, 1985). This is in contrast to dinocysts, which are excellent stratigraphic markers (Heilmann-Clausen and Van Simaeyns, 2005; Köthe, 1990; Köthe and Piesker, 2007; Schjøler, 2005; Van Simaeyns et al., 2005b; Śliwińska et al., 2012) and can also be used for palaeoenvironmental interpretation (Köthe, 1990; Śliwińska et al., 2014b) and palaeoclimatology (Clausen et al., 2012; Van Simaeyns et al., 2005a; Śliwińska et al., 2010; Śliwińska and Heilmann-Clausen, 2011). The Syracuse Oils Norge A/S well 11/10-1 penetrates a remarkably thick lower Oligocene (Rupelian) section in a depocentre (over 600 m; see Jarvese et al., 2015) and is therefore an optimal site for investigating the early icehouse record in mid-latitudes to northern latitudes. Furthermore, the well yields diverse assemblages of well-preserved dinocysts. It is also one of the sites in the North Sea basin penetrating the earliest Oligocene *Svalbardella cooksoniae* interval related to the Oi-1a cooling event (Śliwińska and Heilmann-Clausen, 2011). Thus, it is an excellent candidate for studying the distribution of key dinocyst marker species in the earliest Oligocene and also the climatic impact on the development of the stratigraphic sequences in the North Sea basin. In this paper I aim to (1) present a semi-quantitative study of the dinocysts within this expanded Rupelian succession, (2) provide more refined dinocyst-based ages for the 11/10-1 well, and (3) investigate the climatic impact on the development of the local sequence stratigraphic framework and changes in the dinocyst assemblages related to palaeoenvironmental changes.

2 Study area and site location

The North Sea is an epicontinental basin (Michelsen et al., 1998) located in northern Europe, with a broad connection to the Norwegian Sea to the north and a narrow connection to the North Atlantic Ocean to the southwest via the English Channel (Fig. 1). In the Rupelian the basin was partly enclosed with (i) several shallow, intermittent seaways to the Peritethys, Paratethys and the eastern Atlantic Ocean and (ii) one deep, wide connection to the Norwegian–Greenland Sea that led to the Arctic Ocean (Fyfe et al., 2003; Knox et al., 2010). During the Chattian, the North Sea basin became more isolated from adjacent basins (Knox et al., 2010). Restricted water exchange with the surrounding basins during the Oligocene may explain why planktic foraminifera are extremely rare (e.g. Śliwińska et al., 2012) and why some of the

marker calcareous nannofossil taxa are absent in the southern and eastern North Sea basin (e.g. Van Simaey et al., 2005b; Śliwińska et al., 2014a).

One of the most striking features of the Paleogene succession in the eastern North Sea basin is a rapid change in the sedimentation pattern at the Eocene–Oligocene transition. On seismic cross sections, the Eocene–Oligocene boundary is expressed as a strong and continuous seismic reflector, named top Eocene (e.g. Huuse and Clausen, 2001). The reflector marks the boundary between Eocene hemipelagic calcareous ooze and Oligocene siliciclastic clays. The Oligocene succession in the eastern North Sea basin is divided into four stratigraphic sequences (Danielsen et al., 1997; Jarsve et al., 2015; Michelsen and Danielsen, 1996). Internal clinoform geometry suggests that in the earliest Rupelian (at the boundary of two local seismic sequences, OSS-2 TST and OSS-2 RST, where OSS is the Oligocene seismic sequence, TST is transgressive system tract, and RST is the regressive system tract) the direction of progradation changed from southeast to south and southwest (Jarsve et al., 2015; Fig. 1c). The Syracuse Oils Norge A/S well 11/10-1 was drilled in 1969 in the Norwegian–Danish basin adjacent to the border between the Norwegian and the Danish North Sea sectors (Fig. 1b; coordinates 57°00′46″ N, 6°10′04″ E). The well is located on the western flank of the Horn Graben, close to the Kreps Fault zone (Fig. 1b).

Seismic studies show that the well is in a proximal setting in the lower Oligocene depocentre (e.g. Danielsen et al., 1997; Jarsve et al., 2015). During the Oligocene, the depocentre migrated southwards and basinwards (Danielsen et al., 1997). The mid-Oligocene to late Oligocene depocentre is penetrated by the Nini-1 well (Śliwińska et al., 2010).

3 Previous studies

In the completion report for the 11/10-1 well (NPD_report, 1969b), the interval between 3419 and 3357 ft (i.e. 1042.1 to 1023.2 m) was assigned to the upper Paleocene shale unit. The interval 3357 to 3244 ft (i.e. 1023.2 to 988.8 m) was referred to the upper Paleocene clay and shale unit and between 3244 and 2067 ft (i.e. 988.8 to 630.0 m) to the upper–middle–lower Eocene clay unit, while the interval between 2067 and 900 ft (i.e. 630.0 to ~274.3 to m) was dated as Miocene–Oligocene. In the lithological report for the 11/10-1 well, the interval between 1050 and 1022 m was included in the Rogaland Group, and the interval between 1022 and 305 m was included in the Hordaland Group. The Rogaland Group consists primarily of shale (NPD_report, 1969a). Hordaland Group deposits are predominantly sandy shale. The upper 120 m of the succession consists of sand and sandstone. These sandy deposits are referred to as the Nordland Group, which in the North Sea basin is considered to be middle Miocene to Holocene. Based on foraminiferal assemblages described in the same report, the interval between 1006

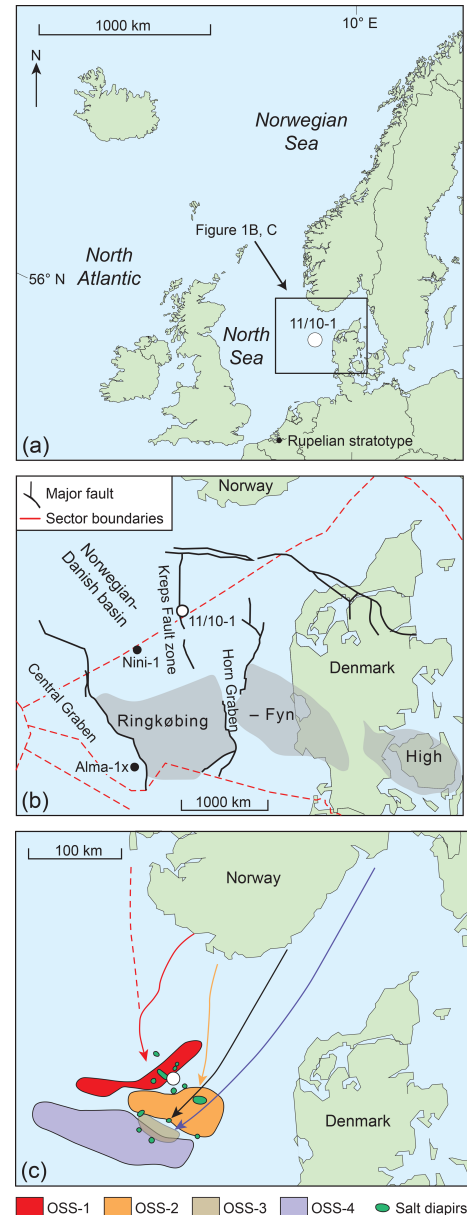


Figure 1. (a) The North Sea basin is located on the eastern flank of the North Atlantic Ocean. The black star marks the location of the Rupelian stratotype (Van Simaey and Vandenberghe, 2006). (b) The 11/10-1 well was drilled close to the border between the Norwegian and the Danish North Sea sectors. Black dots mark the location of two other wells from the North Sea basin which penetrate Oligocene rocks Alma-IX (Schjøler, 2005) and Nini-1 (Clausen et al., 2012; Śliwińska et al., 2010; Śliwińska and Heilmann-Clausen, 2011). (c) The sediment transport direction and the position of the Oligocene depocentres are after Danielsen et al. (1997) and Jarsve et al. (2015). OSS-1 to OSS-4 stand for names of local Oligocene seismic sequences sensu Jarsve et al. (2015). The map shows the distribution of the depocentres for each of the OSS sequence; (a), (b) and (c) are modified from Śliwińska and Heilmann-Clausen (2011), Śliwińska et al. (2010), and Jarsve et al. (2015), respectively.

and 640 m was dated as Oligocene, possibly as the middle Oligocene (see p. 9 therein); the interval from 580 to 305 m was considered to be late Oligocene. Other information concerning the well can be found at <http://factpages.npd.no> (last access: 18 May 2019).

In the early 1990s, the 11/10-1 well was studied under the CENOS project, which aimed to provide a comprehensive sequence stratigraphic study of the Cenozoic of the eastern North Sea basin (e.g. Michelsen et al., 1992, 1998). Based on the 2-D seismic stratigraphy and well logs, Danielsen et al. (1997) recognised four Oligocene seismic sequences within the well (i.e. 4.1–4.4). However, this sequence subdivision was recently challenged by Jarsve et al. (2015), who divided the Oligocene succession from the 11/10-1 well into four alternative regional seismic sequences (OSS-1 to OSS-4; see the comparison of the two sequence stratigraphic frameworks in fig. 3 in Jarsve et al., 2015). Both studies indirectly suggested a Rupelian to middle Chattian age for the succession penetrated by the 11/10-1 well (cf. fig. 4 in Danielsen et al., 1997, and fig. 6 in Jarsve et al., 2015). However, none of these studies clearly define the position of the Rupelian–Chattian boundary.

The first peer-reviewed biostratigraphic framework for the 11/10-1 well was based on semi-quantitative dinocyst analyses (focussing only on the relative abundance of one genus and four dinocyst species) from the lowermost part of the Rupelian succession (914.40–579.10 m b.s.f.; Śliwińska and Heilmann-Clausen, 2011); the Eocene–Oligocene boundary was placed at about 1022 m at the base of sequence 4.1 (Danielsen et al., 1997), equivalent to the top Eocene horizon.

Recently, the age model has been improved with a strontium (Sr) isotope (measured on tests of calcareous foraminifera and mollusc fragments) and micropalaeontological analyses (Eidvin et al., 2013; Jarsve et al., 2015; Fig. 2). As deduced from Figs. 3 and 4 in Jarsve et al. (2015), the Rupelian–Chattian boundary is at ca. 460 m b.s.f. and coincides with the boundary of the two local seismic sequences (i.e. OSS-2 and OSS-3 boundary). The Eocene–Oligocene boundary was not investigated in this study.

4 Material and methods

4.1 Palynology

As mentioned previously, only ditch cutting samples were available from the Paleogene succession of the 11/10-1 well. Samples for palynological slides were collected at ~15 or ~30 m intervals (with one exception where the interval is ca. 45 m; Fig. 3). This study covered local seismic sequences OSS-1 to OSS-3 sensu Jarvese et al. (2015); Fig. 3. I analysed 25 samples (from the interval 914.40 m b.s.f. to 365.2 m b.s.f.), which were processed by the Norwegian Petroleum Directorate (NPD). The laboratory preparation procedure followed standard palynological techniques. Car-

bonates were removed by hydrochloric acid (37 % HCl), and silicates were removed by hydrofluoric acid (40 % HF). Subsequently, pyrite, which was present in the remaining acid-resistant organic residue, was removed by 2 min of oxidation in nitric acid (65 % HNO₃) at room temperature. The organic residue was permanently mounted in Elvacite[®], an acrylic polymer of methyl methacrylate.

To study the Eocene–Oligocene boundary, palynological slides from two additional ditch cutting samples (at 1036.32 and 1005.84 m b.s.f., labelled K-181 and K-180, respectively) were processed at the Institute for Geoscience (IG), Aarhus University (AU), in 2011. The processing techniques were those described in Śliwińska and Heilmann-Clausen (2011).

Transmitted light microscopy was undertaken using a Leica DMR HC microscope. The relative abundance data were obtained by counting at least 300 dinocyst specimens from each sample. The slide was also scanned for rare species. With the exception of the Wetzelielloideae subfamily, treated here as suggested by Bijl et al. (2017), the taxonomic nomenclature of Williams et al. (2017) is applied. Detailed counts of dinocysts are shown in Fig. 3, and the list of encountered species can be found in Table 1. Selected specimens are depicted in Plates 1–8. The position of the photographed specimens on each slide is given in England Finder Coordinate (EFC) system as well as after the new method proposed here (Appendix 1 and Fig. A1). One new species, *Areoligera? barskii* sp. nov., is described, and the morphological variation in *Enneadocysta magna* is discussed in Sect. 7.

4.2 Dinocysts as palaeoenvironmental proxies

The majority of dinoflagellates are marine protists, comprising an important group of the phytoplankton. As primary producers, they are second only to diatoms. In their life cycle, some dinoflagellates produce organic-walled resting cysts (dinocysts), which may be preserved in the geological record (Edwards, 1993). Dinoflagellates are sensitive to many environmental factors, such as sea-surface temperature, salinity, nutrient availability, etc., and thus they can be utilised as environmental proxies. However, only few modern dinocyst genera – e.g. *Impagidinium*, *Lingulodinium*, *Nematosphaeropsis*, *Polysphaeridium* or *Spiniferites* – can be traced back to the late Paleogene. Therefore, while the ecological preferences of Holocene dinocysts are well known (e.g. Zonneveld et al., 2013), most of the pre-Holocene dinocysts are extinct and their environmental affinities are not fully understood. Some of the most common approaches for understanding the palaeoecological preferences of extinct dinocyst taxa are to study the changes in the assemblages across well-established system tracts (e.g. Dybkjær, 2004; Stover and Hardenbol, 1994), study temporal and spatial changes in assemblages (e.g. Damassa and Williams, 1994), or study changes in the assemblages together with palaeoclimatological proxies which can provide information about,

Table 1. Alphabetical list of all identified dinocyst taxa identified in the 11/10-1 well. The first column refers to the position of the taxon in Fig. 3. The right column includes a key for all photographed specimens which are shown in Plates 1 to 8. Rew. stands for reworked.

Position on Fig. 4	Taxa name in alphabetical order according to genus then species	Plate	Photo
20	<i>Achilleodinium biformoides</i>	1	A
21	<i>Achomosphaera</i> spp.	1	B
22	<i>Achomosphaera</i> spp.– <i>Spiniferites</i> spp.		
121	<i>Adnatosphaeridium vittatum</i>	1	K
4	cf. <i>Apteodinium australiense</i>	1	C
143	<i>Alisocysta</i> spp. (reworked)		
144	<i>Apectodinium augustum</i> (reworked)		
145	<i>Apectodinium</i> spp. (reworked)		
60	<i>Apteodinium australiense</i>		
1	<i>Apteodinium spiridoides</i>	1	D
75, 146 (Rew.)	<i>Areoligera senonensis</i> complex sensu Eaton 1976	1	E,F
23	<i>Areoligera</i> spp.		
106	<i>Areoligera tauloma</i>		
57	<i>Areoligera? barskii</i> sp. nov.	8	A-M
124, 147 (Rew.)	<i>Areosphaeridium diktyoplokum</i>	1	I
127	<i>A. diktyoplokum</i> (entire clypeate process terminations)	1	J
125, 148 (Rew.)	<i>Areosphaeridium michoudii</i>	1	G
132	<i>Areosphaeridium</i> spp.		
104	<i>Batiacasphaera</i> spp.		
77	<i>Caligodinium amiculum</i>		
130	<i>Cerebrocysta bartonensis</i>	2	A
101, 149 (Rew.)	<i>Cerebrocysta</i> spp.		
135	<i>Cerodinium depressum</i>		
150	<i>Cerodinium</i> spp. (reworked)		
151	<i>Cerodinium striatum</i> (reworked)		
152	<i>Charlesdownia coleothrypta</i> (reworked)	2	H
153	<i>Charlesdownia columna-edwardsii</i> complex (reworked)	2	G
136, 154 (Rew.)	<i>Charlesdownia</i> spp.		
98	<i>Chiropteridium</i> cf. <i>galea</i>		
24	<i>Chiropteridium galea</i>	2	C
13	<i>Chiropteridium lobospinosum</i>	2	D
86	<i>Chiropteridium</i> spp.		
155	<i>Chlamydophorella nyei</i> (reworked)		
25	<i>Cleistosphaeridium</i> spp.	2	B
26	<i>Cordosphaeridium cantharellus</i>	2	E
131	<i>Cordosphaeridium funiculatum</i>	2	F
85	<i>Cordosphaeridium gracile</i>		
119	<i>Cordosphaeridium inodes</i>		
70	<i>Cordosphaeridium</i> spp.		
88	<i>Corrudinium incompositum</i>		
94	<i>Corrudinium</i> spp.		
27	<i>Cribroperidinium</i> spp.		
28	<i>Dapsilidinium pseudocolligerum</i>	3	A
14	<i>Deflandrea heterophlycta</i>		
137	<i>Deflandrea oebisfeldensis</i> (reworked)	2	K
29	<i>Deflandrea phosphoritica</i>	2	L
30	<i>Deflandrea</i> spp.		
156	<i>Dingodinium cerviculum</i> (reworked)		
31	<i>Dinopterygium cladoides</i>	3	F
138	<i>Diphyes colligerum</i>	3	B
157	<i>Diphyes ficusoides</i> (reworked)		
9	<i>Distatodinium biffii</i>	3	C
10	<i>Distatodinium ellipticum</i>	3	D
32	<i>Distatodinium paradoxum</i>	3	E
33	<i>Distatodinium</i> spp.		

Table 1. Continued.

Position on Fig. 4	Taxa name in alphabetical order according to genus then species	Plate	Photo
115	<i>Dracodinium eoceanicum</i>	7	L
126	<i>Dracodinium samlandicum</i>		
128	<i>Dracodinium</i> spp.		
139, 158 (Rew.)	<i>Eatonicysta ursulae</i>	2	I
47	<i>Enneadocysta magna</i>	3	H,I
61	<i>Enneadocysta pectiniformis</i>	5	A
15	<i>Enneadocysta</i> spp.		
71	<i>Fibrocyta axialis</i>	2	J
129	<i>Fibrocyta</i> spp.		
100	<i>Glaphyrocysta exuberans</i>	4	A
49	<i>Glaphyrocysta microfenestrata</i> – <i>G. texta</i>	4	B,C
122, 159 (Rew.),	<i>Glaphyrocysta semitecta</i>	4	F
102	<i>Glaphyrocysta</i> spp.		
73	<i>Glaphyrocysta vicina</i>	4	E
69	<i>Gochtodinium spinula</i>	4	D
2	<i>Heteraulacacysta campanula</i>		
140, 160 (Rew.)	<i>Heteraulacacysta porosa</i>	4	K
7	<i>Heteraulacacysta pustulata</i>		
95	<i>Heteraulacacysta</i> spp.		
161	<i>Homotryblium caliculum</i>		
11	<i>Homotryblium plectilum</i>		
109	<i>Homotryblium</i> spp.		
34	<i>Homotryblium tenuispinosum</i>		
80	<i>Hystrichodinium</i> spp.		
65	<i>Hystrichokolpoma cinctum</i>	4	H
35	<i>Hystrichokolpoma rigaudiae</i>	4	I
58	<i>Hystrichokolpoma salacia</i>	4	J
53	<i>Hystrichokolpoma</i> spp.		
96	<i>Hystrichosphaeridium</i> spp.		
83	<i>Hystrichosphaeridium tubiferum</i> subsp. <i>tubiferum</i>		
72	<i>Hystrichosphaeropsis obscura</i>	4	G
162	<i>Hystrichostrogylon clausenii</i> (reworked)		
123	<i>Hystrichostrogylon membraniphorum</i>	5	B
50	<i>Hystrichostrogylon</i> spp.		
87	<i>Impagidinium</i> spp.		
120	<i>Impagidinium velorum</i>		
89	<i>Impletosphaeridium insolitum</i>		
90	<i>Lejeunecysta</i> spp.		
112	<i>Lentinia serrata</i>	5	C
48	<i>Licracysta?</i> <i>semicirculata</i>	3	G
36	<i>Lingulodinium machaerophorum</i>	5	D
64	<i>Melitasphaeridium asterium</i>	5	F
116	<i>Melitasphaeridium choanophorum</i>		
133	<i>Melitasphaeridium pseudorecurvatum</i>		
18	<i>Membranophoridium aspinatum</i>	5	I
5	<i>Membranophoridium intermedium</i>		
107	<i>Membranophoridium</i> spp.		
84	<i>Microdinium reticulatum</i>	5	G
54	<i>Minisphaeridium latirictum</i>		
163	<i>Muderongia australis</i> (reworked)		
164	<i>Muderongia</i> spp. (reworked)		
113	<i>Nematosphaeropsis</i> spp.	5	H
165	<i>Odontochitina</i> spp. (reworked)		
108	<i>Oligokolpoma</i> spp.		

Table 1. Continued.

Position on Fig. 4	Taxa name in alphabetical order according to genus then species	Plate	Photo
67	<i>Oligosphaeridium</i> complex		
37	<i>Operculodinium centrocarpum</i>		
111	<i>Operculodinium divergens</i>		
55	<i>Operculodinium microtriainum</i>	5	J
38	<i>Operculodinium</i> spp.		
6	<i>Operculodinium xanthium</i>	5	K
39	Other dinocysts		
62	<i>Palaeocystodinium golzowense</i>		
81	<i>Palaeocystodinium</i> spp.		
79	<i>Palaeocystodinium teespinosum</i>	6	H
166	<i>Palaeoperidinium cretaceum/pyrophorum</i> (reworked)		
167	<i>Palaeoperidinium pyrophorum</i> (reworked)		
103	<i>Pentadinium imaginatum</i>	5	L
16	<i>Pentadinium laticinctum</i>	5	M
40	<i>Pentadinium lophophorum</i>	5	N
78	<i>Pentadinium</i> spp.		
93	<i>Peridinoid</i> dinocyst sp. A	5	E
114	<i>Peridinoid</i> dinocysts		
76	<i>Phthanoperidinium amoenum</i>	6	A
91, 168 (Rew.)	<i>Phthanoperidinium comatum</i>	6	C
59	<i>Phthanoperidinium geminatum</i>	6	B
68	<i>Phthanoperidinium multispinum</i>		
97	<i>Phthanoperidinium</i> spp.		
66, 169 (Rew.)	<i>Phthanoperidinium stockmansii</i>		
92	<i>Polysphaeridium</i> spp.		
170	<i>Pseudoceratium pelliferum</i> (reworked)		
12	<i>Reticulosphaera actinocoronata</i>	6	D
56	<i>Rhombodinium draco</i>	6	I
8	<i>Rhombodinium longimanum</i>	6	J
82	<i>Rhombodinium porosum</i>		
118	<i>Rhombodinium</i> spp.		
117	<i>Samlandia chlamydothora</i>	7	A
52	<i>Spiniferella cornuta</i>		
99	<i>Spiniferites manumii</i>	7	D
41	<i>Spiniferites pseudofurcatus</i>		
42	<i>Spiniferites</i> spp.		
171	<i>Surculosphaeridium</i> spp. (reworked)		
63	<i>Svalbardella cooksoniae</i>	6	E-G
43	<i>Tectatodinium pellitum</i>	7	C
141	<i>Thalassiphora delicata</i>	7	E
110	<i>Thalassiphora fenestrata</i>		
44	<i>Thalassiphora pelagica</i>	7	F-H
105	<i>Thalassiphora</i> spp.		
172	<i>Trithyrodinium</i> spp. (reworked)		
142	<i>Turbiosphaera</i> spp.		
46	Unidentifiable dinocysts		
3	<i>Wetziella articulata</i>	7	K
17	<i>Wetziella gochtii</i>	7	J
74	<i>Wetziella ovalis</i>		
45	<i>Wetziella</i> spp.		
19	<i>Wetziella symmetrica</i>	7	I

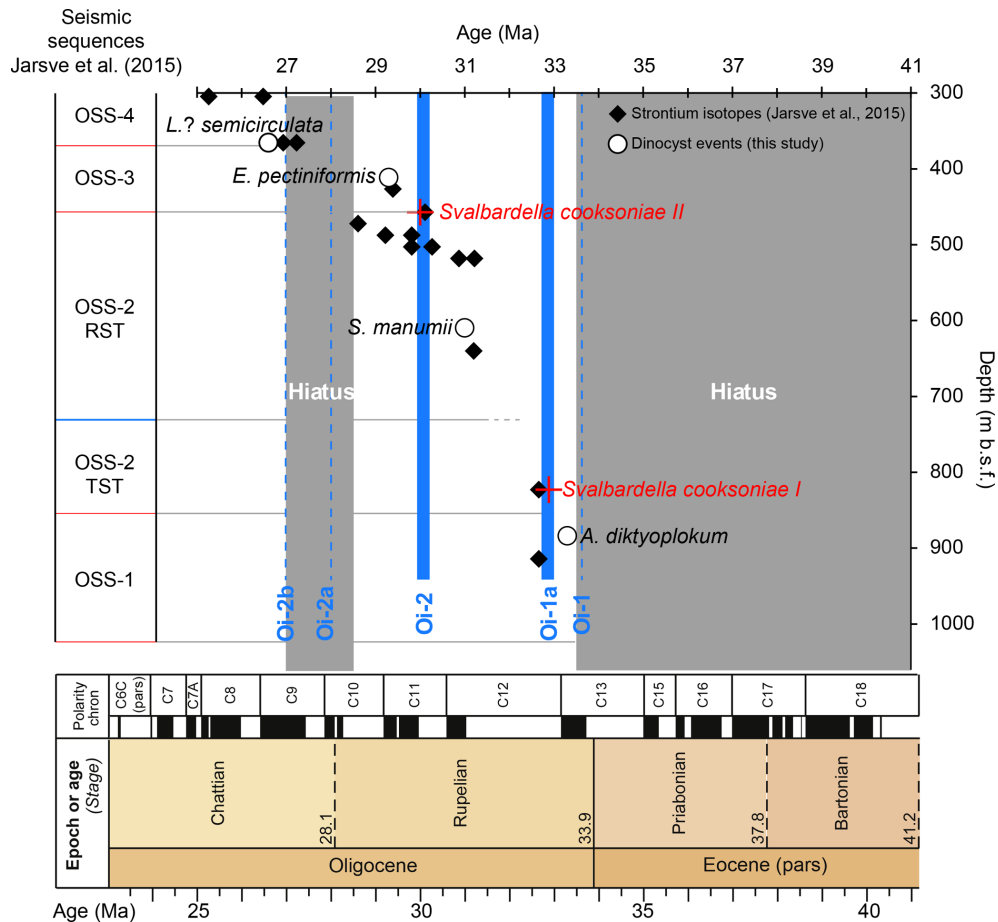


Figure 2. The updated age model for the 11/10-1 well and the time span of possible hiatuses. The dinocyst events (white circles; this study) and strontium (Sr) isotopes (black diamonds; Jarsve et al., 2015) are plotted against the GTS2012 (Vandenberghe et al., 2012). The position of the Oi events against the polarity zones is based on the $\delta^{18}\text{O}$ record from ODP Site 1218; the Oi-1 and the Oi-1a are plotted after Galeotti et al. (2016), while Oi-2, Oi-2a and Oi-2b are plotted after Wade and Pälike (2004). Even if the base Chattian is now positioned in the lower part of C9n (Coccioni et al., 2018), the hiatus in well 11/10-1 will still span the Rupelian–Chattian boundary. Dinocyst events consist of last occurrences (LOs) which are dated as follows: the LO of *Licracysta? semicirculata* – 28.5 Ma (Williams et al., 2004), the LO of *Enneadocysta pectiniformis* – 29.3 Ma (Williams et al., 2004), the LO of *Spiniferites manumii* – 30.8 Ma (Eldrett et al., 2004) – the LO of *Areosphaeridium diktyoplokum* – 33.3 Ma (Eldrett et al., 2004).

for example, sea surface temperature (e.g. Bijl et al., 2011). However, palaeoenvironmental interpretations of some of the pre-Holocene dinocysts are inconsistent and contradictory (Śliwińska et al., 2014a; Woods et al., 2014). What is more, the study by Stover and Hardenbol (1994) investigating the distribution pattern of various dinocyst eco-groups within lower Oligocene sequences in the Rupelian stratotype region suggested that higher concentrations of the most abundant groups show little relationship to system tracts. Nevertheless, despite uncertainties, the understanding of the spatial distribution of dinocysts in past environments is constantly improving, so I will attempt to correlate trends with the existing sequence stratigraphic framework. Selected environmental dinocyst groups discussed in the text are listed in Table 1. Dinocysts can be applied as a proxy for surface water productivity. This is estimated as the ratio between heterotrophic

and autotrophic dinocysts ($P/P+G$), where P is the number of peridinioid dinocysts and G is the number of gonyaulacoid cysts. This is based on the assumption that all peridinioid cysts are derived from heterotrophic dinoflagellates which feed on diatoms, while gonyaulacoid cysts mainly represent dinoflagellates which are autotrophs (Powell et al., 1992). Even though this approach has some weaknesses (see discussion in, for example, Sluijs et al., 2005), the $P/P+G$ ratio has successfully been applied in numerous palaeoenvironmental studies (e.g. Eshet et al., 1994; De Schepper et al., 2009; Versteegh, 1994).

5 Results and discussion

All samples yielded diverse and rich dinocyst assemblages. Within the assemblages, acritarchs (e.g. *Cyclop-*

Well 11/10-1

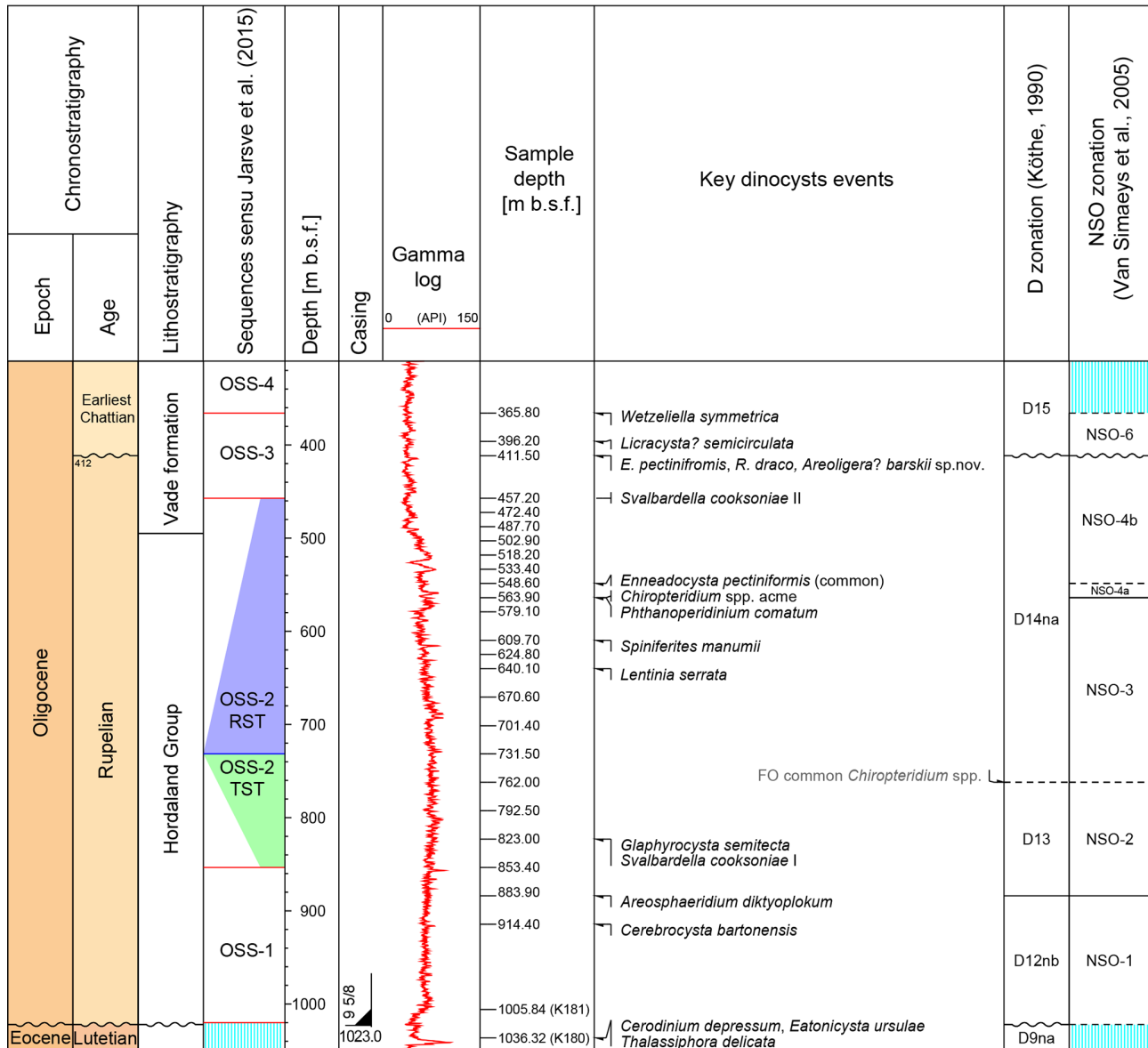


Figure 3. Chronostratigraphy (this study), lithostratigraphy and sequence stratigraphy (Jarsve et al., 2015), depth scale, casing and the gamma log of the studied succession in the 11/10-1 well are followed by key dinocyst events, the dinocyst zonal subdivision and the position of the studied samples (this study).

siella elliptica), Prasinophytes (e.g. *Cymatiosphaera bujakii* – Plate 1H), brackish to freshwater algae (*Botryococcus* spp. – Plate 2L; *Pediastrum* spp.) and terrestrial sedimentary particles (wood, plant tissues, pollen and spores; not quantified in the present study) occur sporadically. The preservation of dinocysts is good to excellent; 162 dinocyst taxa are identified to the species or genus level (Fig. 4). One new species, *Areoligera? barskii* sp. nov., is described (see Sect. 7), and the morphological variation within *Enneadocysta magna* is discussed (Sect. 7). Studied assemblages contain some of the most important age-dagnostic dinocysts, including

the following: *Areosphaeridium diktyoplokum*, *Chiropteridium galea*, *Chiropteridium lobospinosum*, *Distatodinium bifii*, *Enneadocysta pectiniformis*, *Glaphyrocysta semitecta*, *Lentinia serrata*, *Licracysta? semicirculata*, *Phthanoperidinium comatum*, *Rhombodinium draco*, *Spiniferites manumii*, *Wetzeliella gochtii* and *Wetzeliella symmetrica*. In addition to the earliest Rupelian *Svalbardella cooksoniae* interval (*Svalbardella cooksoniae* I; 883.90–823.00 m b.s.f.), I recorded a second, slightly younger interval of *Svalbardella cooksoniae* between 518.20 and 457.20 m b.s.f. (*Svalbardella cooksoniae* II; Figs. 2 and 3). The dinocyst assemblages show

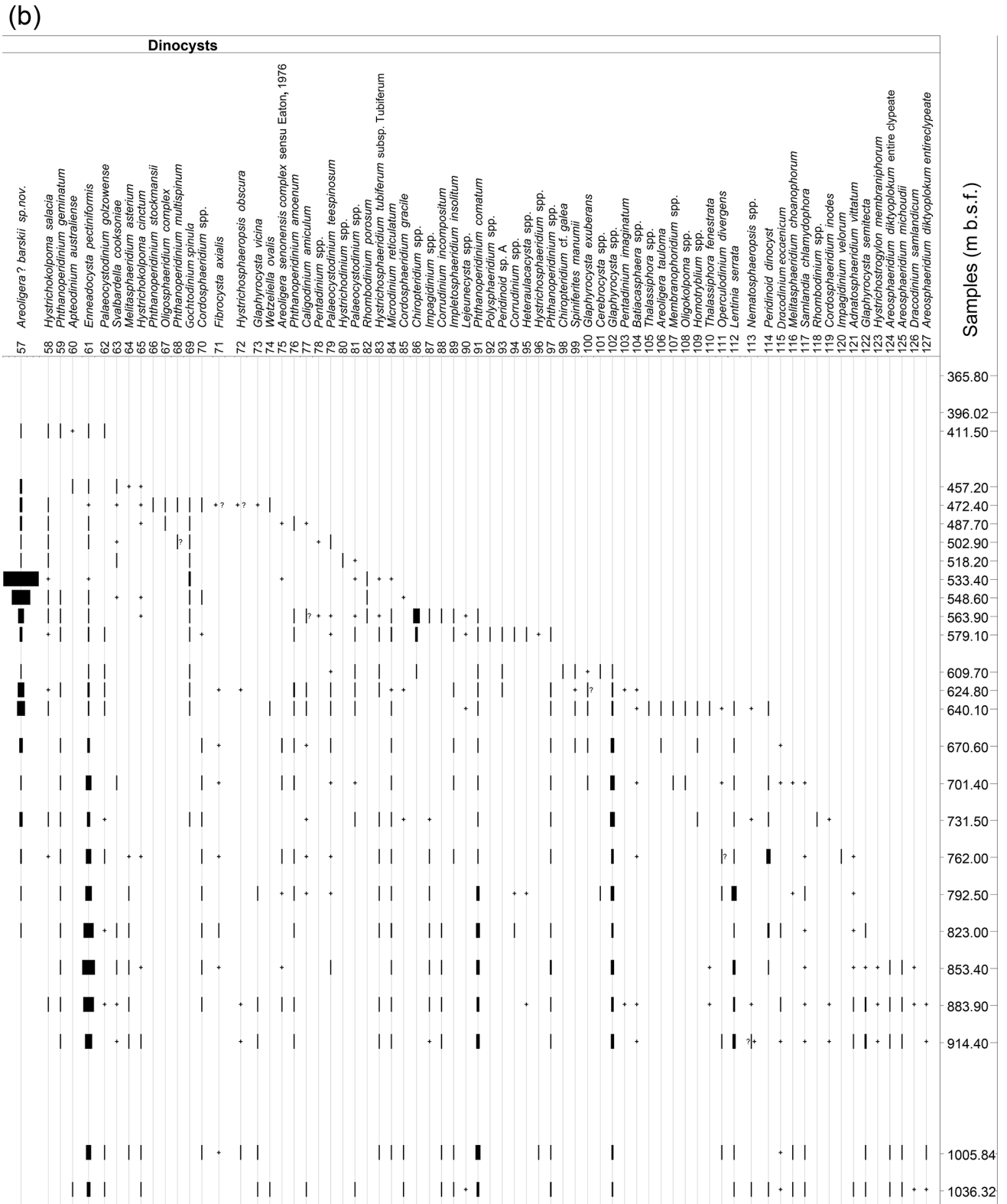


Figure 4.

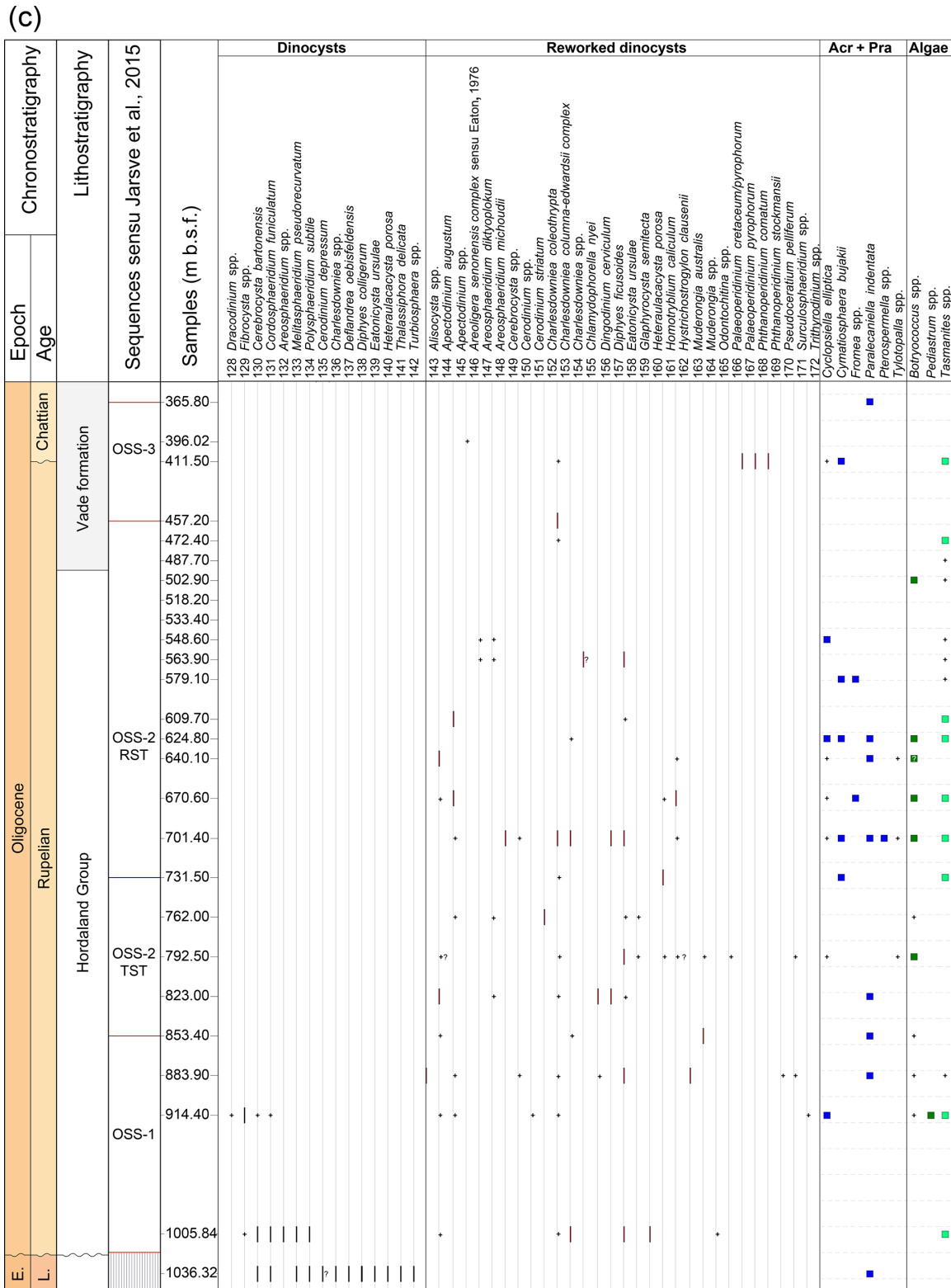


Figure 4. Range chart showing the relative abundance (%) of all recorded dinocysts (in situ and reworked) and presence and absence record of acritarchs and algae (number of specimens observed within the counting area). The distribution of the dinocysts in the 11/10-1 well is arranged according to the last occurrence (LO), while acritarchs and algae are arranged alphabetically. E. – Eocene; L. – Lutetian. Acr+Pra – acritarchs and Prasinophytes.

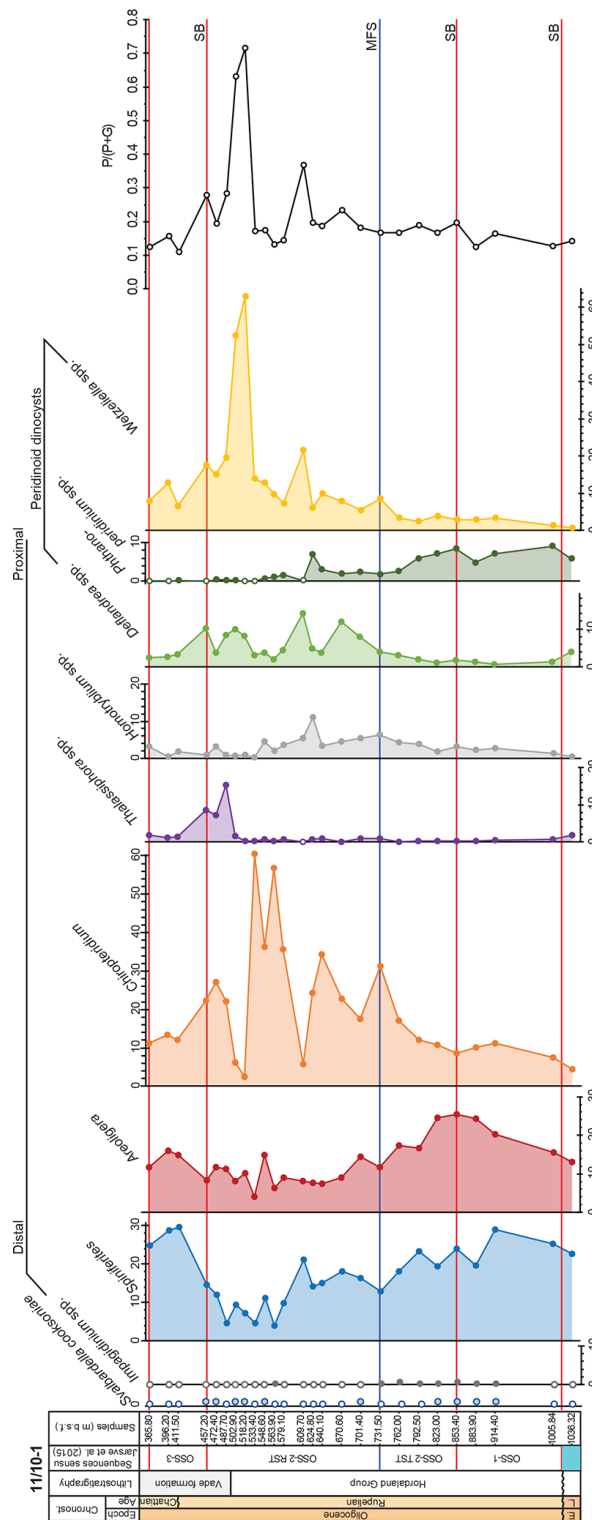


Figure 5. The relative abundance (%) of selected dinocysts groups recorded in the studied interval of the 11/10-1 well plotted against the sequence stratigraphic framework (Jaršve et al., 2015). Red horizontal lines marks sequence boundaries, and the blue line marks maximum flooding surface. All samples with “0” values are marked with dots with white filling.

great abundance and variety within the studied succession (Figs. 4 and 5), considered to be reflecting highly dynamic palaeoenvironmental changes. The three most abundant taxa include *Areoligera? barskii* sp. nov. (up to ~ 55 % of the total dinocyst assemblage), *W. symmetrica* (up to ~ 45 % of the total dinocyst assemblage) and *C. lobospinosum* (up to 30 % of the total dinocyst assemblage). Reworking of Cretaceous (e.g. *Muderongia australis* and *Odontochitina* sp.) and Eocene and Paleocene (e.g. *Eatonicysta ursulae*, *Diphyes ficusoides* and *Apectodinium augustum*) taxa occurs throughout the succession. Reworking is more common in the OSS-1, OSS-2 TST and the lower part of the OSS-2 RST, although overall reworked taxa make up less than 1.5 % of the total dinocyst assemblage (Fig. 4). In the 11/10-1 well, there are no palynological slides available from the samples above 365.76 m b.s.f. (1200 ft; <http://factpages.npd.no>, last access: 18 May 2019) to evaluate the degree of caving from the post-Oligocene deposits. However, downhole contamination and caving from the overlying, possibly middle Miocene to Holocene (see Sect. 3) deposits is regarded as negligible because (i) the casing at 253.0 m b.s.f. should preclude downhole contamination from the overlying strata and (ii) the post-Oligocene deposits consist of medium- to coarse-grained sandstone (NPD_report, 1969b). Due to the high-energy, nutrient-poor environment during deposition of sandy deposits, dinocysts are usually absent (e.g. Dybkjær et al., 2019).

5.1 Dinocyst stratigraphy

5.1.1 Oligocene age framework based on dinocysts

As this study is based on ditch cutting samples, the ages are based primarily on the last or youngest stratigraphic occurrence (LO) of dinocyst taxa.

The LO of *Areosphaeridium diktyoplokum* is an important earliest Rupelian marker (e.g. Köthe, 1990; Van Mourik and Brinkhuis, 2005; Van Simaëys et al., 2005b). This species has a stratigraphic range of middle Eocene to earliest Oligocene (Heilmann-Clausen and Van Simaëys, 2005; Köthe and Piesker, 2007), but the taxon is often found reworked in younger Oligocene deposits together with other (also reworked) pre-Oligocene dinocysts (e.g. Eldrett et al., 2004; Śliwińska et al., 2012). Onshore in Denmark the LO of *A. diktyoplokum* is observed within the lower C12r chronozone (Śliwińska et al., 2012). In all hitherto studied offshore wells from the North Sea basin, i.e. Nini-1, Alma-1X and Mona-1 (Schiøler, 2005; Śliwińska and Heilmann-Clausen, 2011), the LO of this taxon is located at or just above the top Eocene unconformity, which spans the Eocene–Oligocene boundary (Schiøler, 2005; Śliwińska and Heilmann-Clausen, 2011). In the 11/10-1 well *A. diktyoplokum* occurs persistently in the five lowermost samples (between 853.40 and 1036 m b.s.f.). The top of the persistent occurrence is at 853.40 m b.s.f., although in this sample only one com-

plete specimen (and a couple of opercula) was recorded. At 886.90 m b.s.f. there were six specimens of *A. diktyoplokum* (including two within the counting area), one of which having notably entire clypeate process terminations (for an overview of processes in *A. diktyoplokum*, see, e.g. Fensome et al., 2006). In Denmark, *A. diktyoplokum* specimens from the lower and middle Eocene typically have ragged clypeate process terminations (Heilmann-Clausen, personal communication, 2011 see also Śliwińska, 2011), in contrast to the specimens from the earliest Rupelian (the Viborg Formation), which are characterised by entire clypeate process terminations. Specimens of *A. diktyoplokum* with both entire and ragged processes occur in the Oligocene of well 11-10-1 and in the lowermost sample considered to be middle Eocene (see below).

Nevertheless, the LO of in situ *A. diktyoplokum* is placed at 883.90 m b.s.f. because at that depth several specimens were observed, including one with entire clypeate process terminations. All specimens of *A. diktyoplokum* above 883.90 m b.s.f. are considered to be reworked. Placing *A. diktyoplokum* at 883.90 m b.s.f. implies that its LO is over 130 m above the Eocene–Oligocene boundary (equivalent to the top Eocene seismic horizon; see above). In the stratotype area for the Eocene–Oligocene boundary (in the Massicore borehole), the thickness of the interval between the Eocene–Oligocene boundary horizon and the LO of *A. diktyoplokum* is ~ 6.5 m (Van Mourik and Brinkhuis, 2005), whereas in an expanded upper Eocene to lower Oligocene succession from the western North Atlantic, the thickness is ~ 15 m (Egger et al., 2016). Furthermore, correlation with the Nini-1 well (Fig. 6), which penetrates almost 1 km of Oligocene strata, shows that the Rupelian succession in 11/10-1 is significantly thicker.

From 411.5 to 823.00 m b.s.f., the following Rupelian LOs were recorded: *Phthanoperidinium comatum* (at 563.90 m b.s.f.), *Lentinia serrata* (at 640.10 m b.s.f.), *Spiniferites manumii* (at 609.70 m b.s.f.) and *Glaphyrocysta semitecta* (at 823.00 m b.s.f.; Fig. 3). The LOs of *P. comatum*, *S. manumii* and *L. serrata* occur in the same stratigraphic order as in the western North Atlantic, where the events were dated to 30.7, 31.6 and 33.3 Ma, respectively (cf. Egger et al., 2016). Despite the risk of caving, it is noted that the interval of *S. manumii* in 11/10-1 is relatively thin (~ 60 m; the lowermost sample yielding *S. manumii* is at 670.60 m b.s.f.). This is in agreement with the stratigraphic range of *S. manumii* given previously by Śliwińska and Heilmann-Clausen (2011). The narrow range of *S. manumii* in the North Atlantic region (Egger et al., 2016; Eldrett et al., 2004; Lund, 2002; Williams and Manum, 1999) makes the taxon an excellent mid-Rupelian marker. The top of persistent occurrence of *G. semitecta* occurs at 823.00 m b.s.f., indicating that the LO of this species is one sample higher than suggested by Śliwińska and Heilmann-Clausen (2011). Previous studies suggest that in the eastern North Sea basin (Śliwińska et al., 2012) and Tethys (Van Mourik and Brinkhuis,

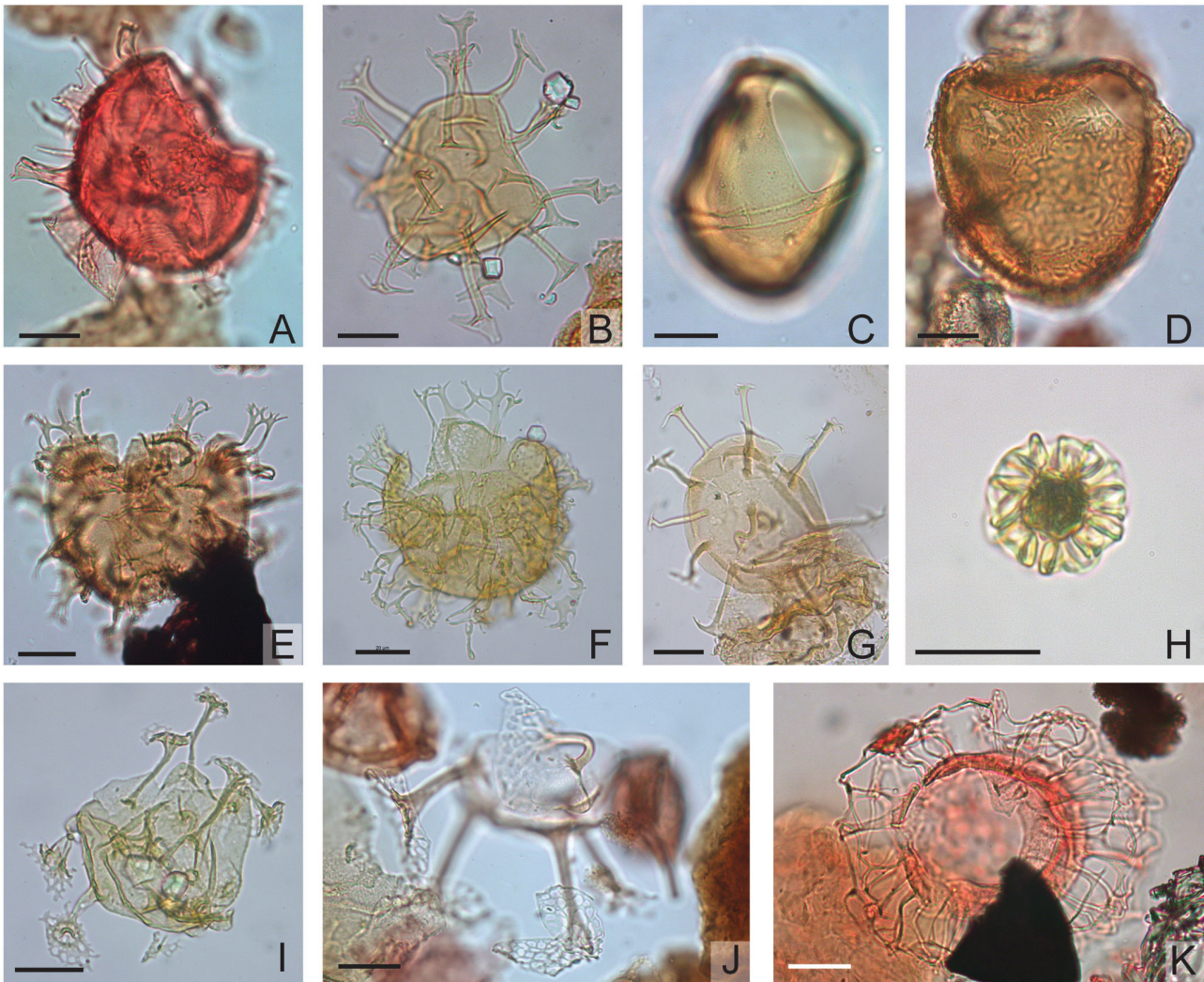


Plate 1. Scale bar of 20 μm applies to all figures; all photographs taken using differential interference contrast. EFC is England. Finder Coordinate; MC is microscope coordinate. If not stated otherwise, the taxon is shown in dorsoventral view. **(A)** *Achilleodinium biformoides*: depth 1036.32 m b.s.f., slide K-180, F-2, EFC J52, MC 51.4 \times 107; left lateral view. **(B)** *Achomosphaera ramulifera*: depth 823.00 m b.s.f., slide \varnothing 1/4', EFC M29/4, MC 29.5 \times 103; left lateral view. **(C)** Aff. *Apteodinium australiense*: depth 365.80 m b.s.f., slide \varnothing 2', EFC D54, MC 31.2 \times 106.7; oblique left lateral view. **(D)** *Apteodinium spiridoides*: depth 365.80 m b.s.f., slide \varnothing 2', EFC J31, MC 32.2 \times 106.7; oblique left lateral view. **(E)** *Areoligera senoniensis* complex sensu Eaton 1976: depth 487.70 m b.s.f., slide \varnothing 2', EFC J39/3, MC 38.7 \times 106.2. **(F)** *Areoligera senoniensis* complex sensu Eaton 1976: depth 670.70 m b.s.f., slide \varnothing 1/4', EFC Q64/1, MC 62.9 \times 100.3; oblique. **(G)** *Areosphaeridium michoudii*: depth 1036.32 m b.s.f., slide K180, F-2, EFC B49/1, MC 48 \times 113.5. **(H)** Prasinophytes *Cymatiosphaera bujakii*: depth 624.80 m b.s.f., slide \varnothing 1/4', EFC L40/4, MC 40 \times 104.4. **(I)** *Areosphaeridium diktyoplokum* with rigged clypeate process terminations: depth 883.90 m b.s.f., slide \varnothing 1/4', EFC G29/2, MC 29.8 \times 109. **(J)** *Areosphaeridium diktyoplokum* with entire clypeate process terminations: depth 1005.84 m b.s.f., slide K-181, F-3, EFC D42/1, MC 41 \times 111.5. **(K)** *Adnatosphaeridium vittatum*: depth 1036.32 m b.s.f., slide K-180, F-2, EFC R47, MC 47 \times 99; oblique polar view.

2005), the LO of *G. semitecta* occurs in the early Chron C12r. In 11/10-1 the sample at 823.00 m b.s.f. yielding the LO of *G. semitecta* has a strontium isotopic age of 32.59 Ma (based on 19 foraminifera tests; Jarsve et al., 2015), and the LO of *Svalbardella cooksoniae* is related to the Oi-1a cooling event (early C12r; Pekar and Miller, 1996). This age constraint implies that in the 11/10-1 well, the event also falls within the

early Chron C12r and thus confirms the synchronism of the event between the eastern North Sea basin and the Tethys.

Two important markers for the Rupelian–Chattian boundary in the North Sea basin, *Rhombodinium draco* and *Enneadocysta pectiniformis* (Schjøler, 2005; Śliwińska et al., 2012; Van Simaey et al., 2005b), occur in the sample at 411.50 m b.s.f. In the southern and eastern North Sea basin, the LO of *R. draco* is known from the earliest Chattian

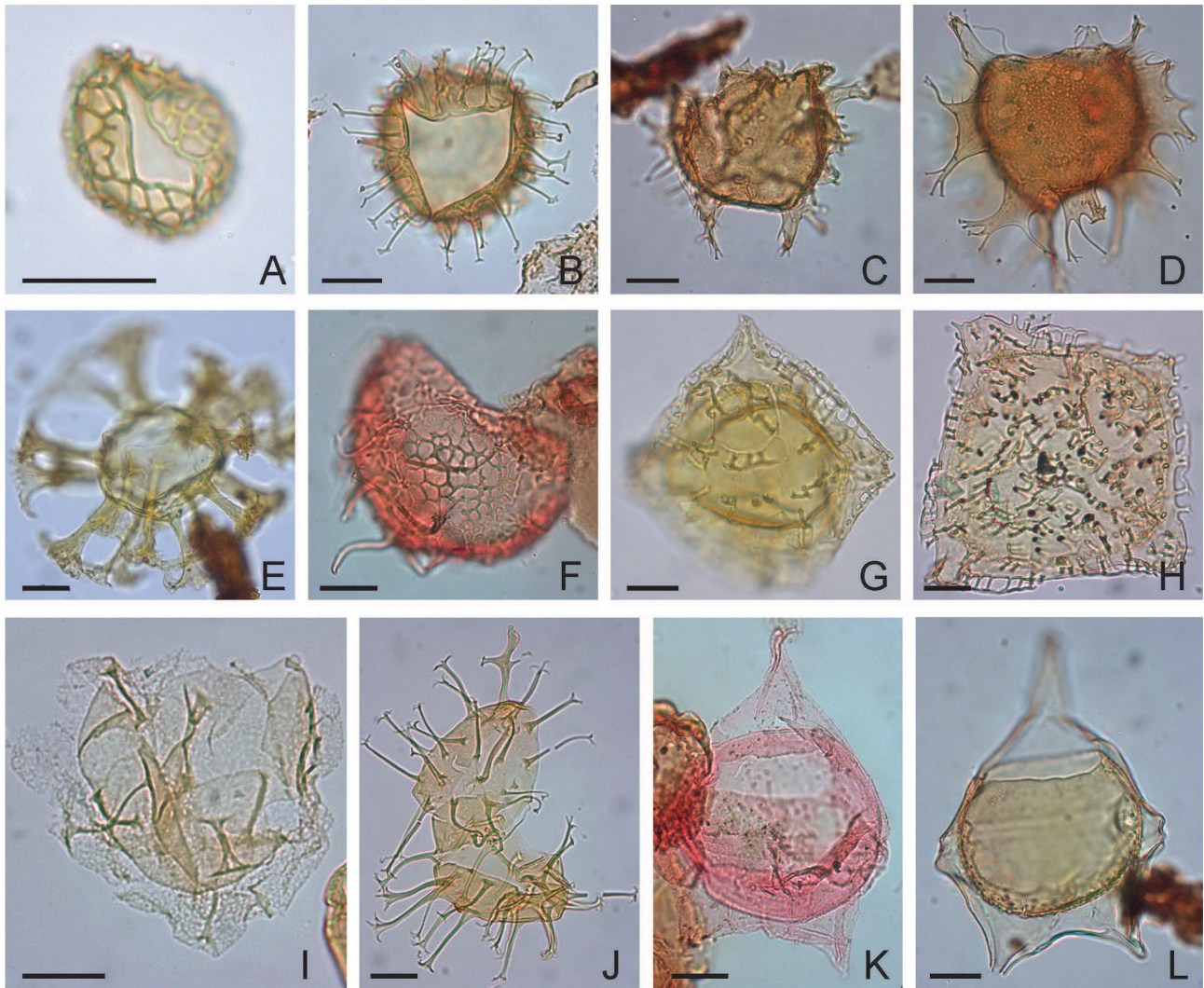


Plate 2. (A) *Cerebrocysta bartonensis*: depth 914.40 m b.s.f., slide \varnothing 1/4', EFC K49/2, MC 48.5 \times 106. (B) *Cleistosphaeridium* spp.: depth 411.50 m b.s.f., slide \varnothing 2', EFC O25, MC 25 \times 101.7; polar view. (C) *Chiropteridium galea*: depth 396.2 m b.s.f., slide \varnothing 2', EFC M37, MC 36.8 \times 103.8. (D) *Chiropteridium lobospinosum*: depth 487.70 m b.s.f., slide \varnothing 2'. (E) *Cordosphaeridium cantharellus*: depth 640.10 m b.s.f., slide \varnothing 1/4', EFC M39/1, MC 38.5 \times 103.9. (F) *Cordosphaeridium funiculatum*: depth 1005.84 m b.s.f., slide K-181, F-3, EFC J31/2, MC 31.3 \times 106.8; oblique left lateral view. (G) Reworked *Charlesdownia columna-edwardsii* complex: depth 883.90 m b.s.f., slide \varnothing 1/4', EFC T36, MC 35.8 \times 97. (H) *Charlesdownia coleothrypta*: depth 472.40 m b.s.f., slide \varnothing 2', EFC T66, MC 64.6 \times 97; rotated 45° clockwise. (I) Reworked *Eatonicysta ursulae*: depth 883.90 m b.s.f., slide \varnothing 1/4', EFC L61/4, MC 60.5 \times 104.5. (J) *Fibrocysta axialis*: depth 762.00 m b.s.f., slide \varnothing 1/4', EFC W37/2, MC 37.5 \times 94. (K) Reworked *Deflandrea oebisfeldensis*: depth 1036.32 m b.s.f., slide K-180, F-2, EFC K22/4, MC 22.8 \times 105. (L) *Deflandrea phosphoritica*: depth 365.80 m b.s.f., slide \varnothing 2', EFC D54, MC 53.2 \times 111.2.

(Köthe, 1990; Śliwińska et al., 2012; Van Simaey et al., 2005b). This event should, however, be applied with caution, since its last stratigraphic occurrence seems to be diachronous across Europe (Pross, 2001a). In the western North Atlantic and the western Tethys, the LO of *E. pectiniformis* is early Chattian (Egger et al., 2016; Pross et al., 2010), in contrast to the North Sea basin, where it occurs persistently in the latest Rupelian (Köthe, 1990; Śliwińska et al., 2012; Van Simaey et al., 2005b). The LOs of *R. draco* and *E. pectiniformis* in well 11/10-1 in the same sample

at 410.5 m b.s.f. suggest that the Rupelian–Chattian boundary is located somewhere close to that depth. This level is also considered to coincide with an unconformity or a condensed section. The revised age determinations therefore position the boundary slightly higher than suggested by Jarsve et al. (2015; Fig. 3). Jarsve et al. (2015) suggested that the Rupelian–Chattian boundary coincides with the local seismic sequence boundary (i.e. the OSS-2–OSS-3 boundary), located around 455 m b.s.f. according to Fig. 4 in Jarsve et al. (2015).

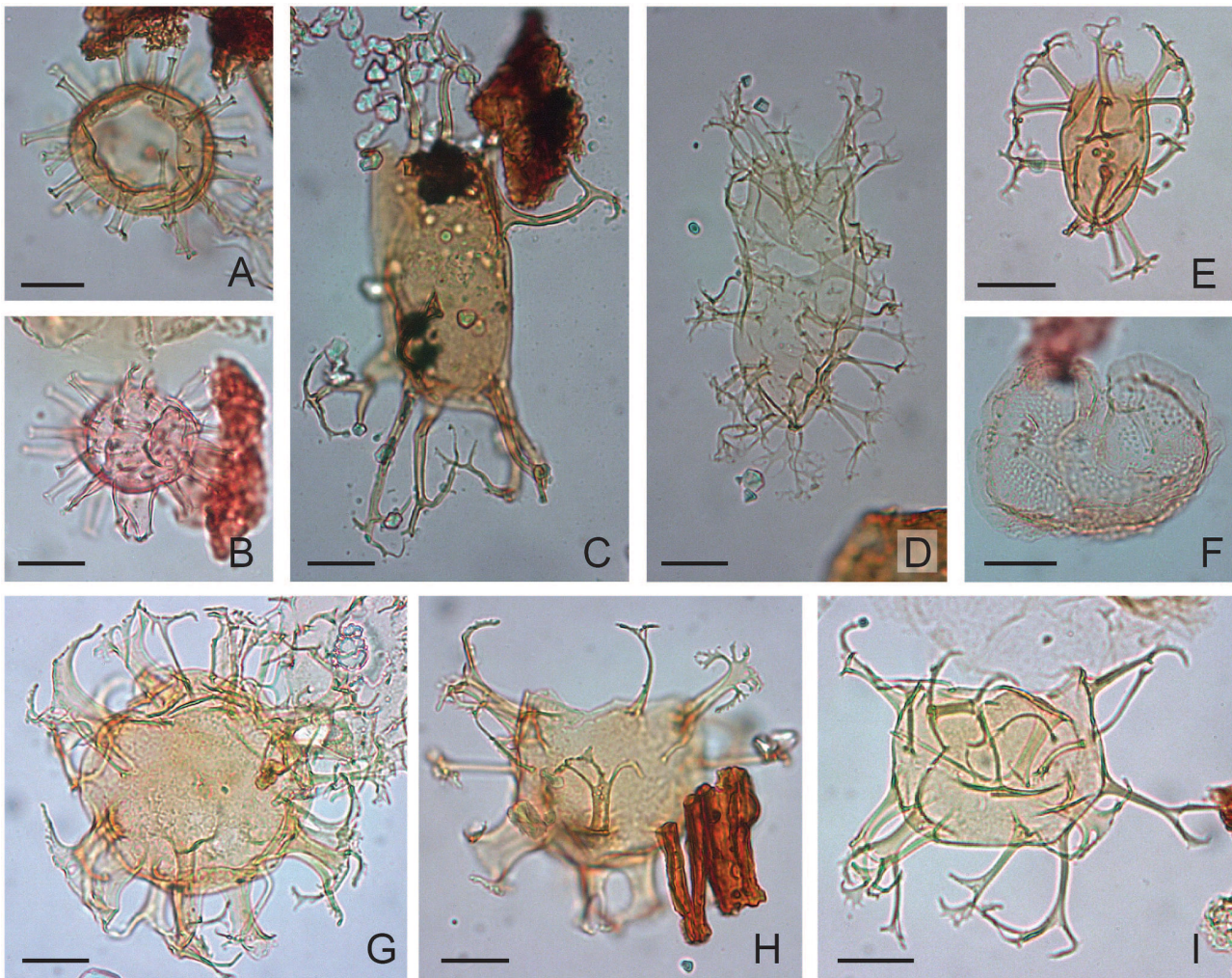


Plate 3. (A) *Dapsilidinium pseudocolligerum*: depth 396.20 m b.s.f., slide \varnothing 2', EFC N34, MC 34 \times 102.9; polar view. (B) *Diphyes colligerum*: depth 1036.32 m b.s.f., slide K-180, F-2, EFC P49, MC 48.5 \times 101. (C) *Distatodinium biffii*: depth 365.80 m b.s.f., slide \varnothing 2', EFC U70, MC 69 \times 97.2. (D) *Distatodinium ellipticum*: depth 563.90 m b.s.f., slide \varnothing 1/4', EFC L41/1, MC 40.5 \times 105. (E) *Distatodinium paradoxum*: depth 365.80 m b.s.f., slide \varnothing 2', EFC M61/4, MC 60.4 \times 103.5. (F) *Dinopterygium cladoides*: depth 1005.84 m b.s.f., slide K-181, F-3, EFC G32/3, MC 31.8 \times 108; polar view. (G) *Licracysta? semicirculata*: depth 472.40 m b.s.f., slide \varnothing 1/4', EFC P45/3, MC 44.7 \times 100.3. (H) A transitional form between *E. magna* and *L.? semicirculata*: depth 411.50 m b.s.f., slide \varnothing 2', EFC D51/3, MC 50 \times 111.4. (I) *Enneadocysta magna*: depth 472.40 m b.s.f., slide \varnothing 1/4', EFC M58, MC 57.3 \times 103.8.

The LO of *Licracysta? semicirculata* at 396.20 m b.s.f. followed by the presence of *Chiropteridium galea*, *Chiropteridium lobospinosum*, *Distatodinium biffii*, *Wetzeliella gochtii* and *Wetzeliella symmetrica* at 365.8 m b.s.f. (the topmost sample; Fig. 3) suggests that the age of the uppermost part of the studied succession is earliest Chattian (e.g. Dybkjær and Rasmussen, 2007; Köthe and Piesker, 2007; Pross et al., 2010; Schiøler, 2005; Van Simaeyns et al., 2005b; Śliwińska et al., 2012; Williams and Manum, 1999). The persistent presence of *Operculodinium xanthium* between 701.40 and 365.8 m b.s.f., i.e. in the interval considered as latest Rupelian to earliest Chattian, suggests that the range of the

taxon in well 11/10-1 is similar to that reported from Germany (Köthe and Piesker, 2007; Fig. 4).

The correlation between the 11/10-1 and the Nini-1 wells is based on a number of dinocyst events (Fig. 6), including the LO of *Enneadocysta pectiniformis*, the LO of common *E. pectiniformis*, an acme of *Chiropteridium* spp., the LO of *Phthanoperidinium comatum*, the LO of *Spiniferites manumii*, the LO of *Glaphyrocysta semitecta* and the LO of *A. diktyoplokum*. This correlation clearly illustrates the expanded character of the Rupelian succession in the 11/10-1 well, indicating that this well represents the thickest lowest Oligocene succession known. Based on the two datums, the LO of *A. diktyoplokum* at 883.90 m b.s.f. (\sim 33.3 Ma) and the

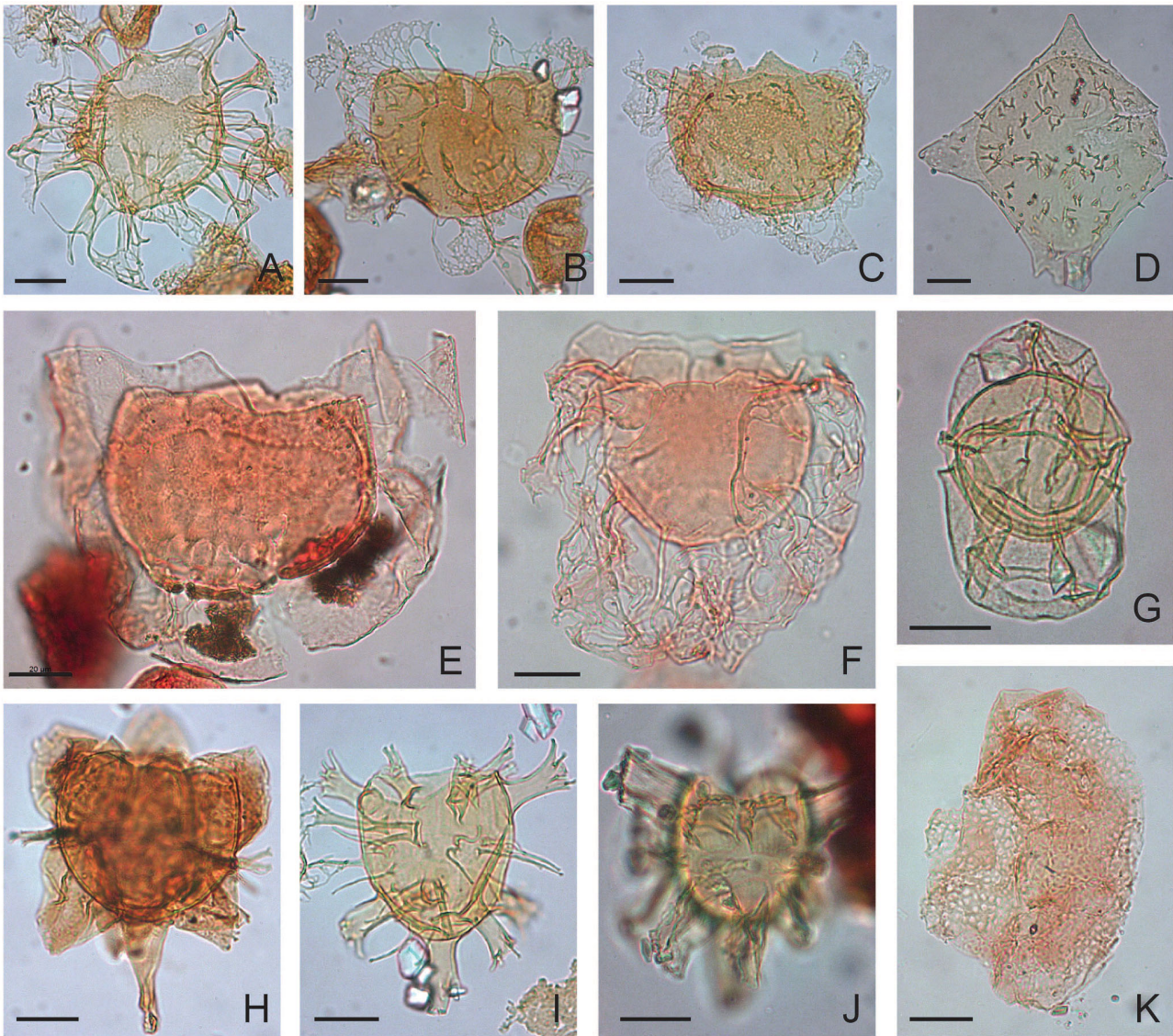


Plate 4. (A) *Glaphyrocysta? exuberans*: depth 624.80 m b.s.f., slide \varnothing 1/4', EFC L29/4, MC 29.5 \times 104. (B) *Glaphyrocysta microfenestrata-texta* complex: depth 792.50 m b.s.f., slide \varnothing 1/4', EFC L20/1, MC 20.3 \times 105. (C) *Glaphyrocysta microfenestrata-texta* complex: depth 609.70 m b.s.f., slide \varnothing 1/4', EFC K23/4, MC 29 \times 105. (D) *Gochtodinium spinula*: depth 472.4 m b.s.f., slide \varnothing 1/4', EFC L43/1, MC 42.3 \times 105. (E) *Glaphyrocysta? vicina*: depth 1005.84 m b.s.f., slide K-181, F-3, EFC L25, MC 25.5 \times 104.8. (F) *Glaphyrocysta semitecta*: depth 1036.32 m b.s.f., slide K-180, F-2, EFC Q59, MC 58.5 \times 100. (G) *Hystrichosphaeropsis obscura*: depth 472.4 m b.s.f., slide \varnothing 1/4', EFC R42, MC 42 \times 98.7. (H) *Hystrichokolpoma cinctum*: depth 457.20 m b.s.f., slide \varnothing 2', EFC V56, MC 55.5 \times 94.8. (I) *Hystrichokolpoma rigaudiae*: depth 762.00 m b.s.f., slide \varnothing 1/4', EFC N26/2, MC 26.3 \times 103. (J) *Hystrichokolpoma salacia*: depth 411.50 m b.s.f., slide \varnothing 2', EFC N23/3, MC 23 \times 102.3. (K) Caved *Heteraulacacysta porosa*: depth 1036.32 m b.s.f., slide K-180, F-2, slide \varnothing 1/4', EFC P59, MC 58.7 \times 101; polar view.

LO of *E. pectiniformis* at 411.50 m b.s.f. (29.3 Ma), the approximate average sedimentation rate for the Rupelian succession is estimated as ~ 12 cm kyr⁻¹.

5.1.2 Local dinocyst (D and NSO) zonations

The two most commonly applied dinocyst zonations for the Oligocene in the North Sea basin (i.e. the dinocyst (D-) zonation

of Costa and Manum, 1988, redefined by Köthe, 1990; and the North Sea Oligocene (NSO-) dinocyst zonation defined by Van Simaey et al., 2005b) were based on sediment cores and outcrop sections from the southern North Sea (Fig. 7). The two zonations utilise both first (FO) and last (LO) stratigraphic occurrences. As mentioned above, this study was restricted to ditch cutting samples. Due to downhole contamination (caving) it is difficult to recog-

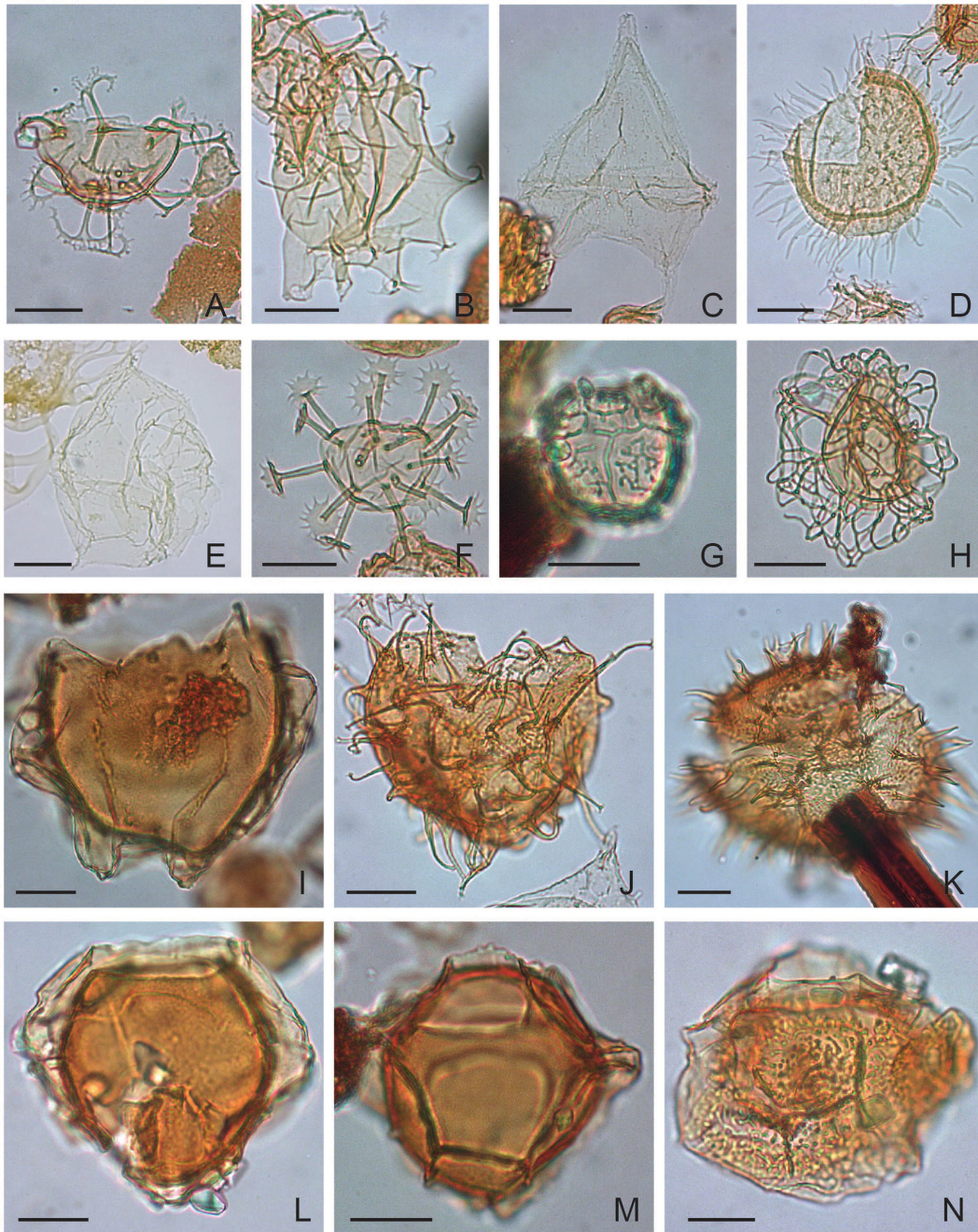


Plate 5. (A) *Enneadocysta pectiniformis*: depth 624.80 m b.s.f., slide \varnothing 1/4', EFC N32/1, MC 103.1 \times 31.8. (B) *Hystrichostrogylon membraniphorum*: depth 701.40 m, slide \varnothing 1/4', EFC M52/1, MC 51.2 \times 104; oblique right lateral view. (C) *Lentinia serrata*: depth 762.00 m b.s.f., slide \varnothing 1/4', EFC T36, MC 35.7 \times 97. (D) *Lingulodinium machaerophorum*: depth 823.00 m b.s.f., slide \varnothing 1/4', EFC L29, MC 29 \times 104.5; oblique right lateral view. (E) Peridinoid cyst sp. A: depth 609.70 m b.s.f., slide \varnothing 1/4', EFC M30, MC 30.3 \times 103.6. (F) *Melitasphaeridium asterium*: depth 762.00 m b.s.f., slide \varnothing 1/4', EFC H58, MC 57 \times 107.7. (G) *Microdinium reticulatum*: depth 563.90 m b.s.f., slide \varnothing 1/4', EFC L66/3, MC 64.6 \times 104.4. (H) *Nematospaeropsis labyrinthus*: depth 914.40 m b.s.f., slide \varnothing 1/4', EFC L42/4, MC 42.2 \times 104.4. (I) *Membranophoridium aspinatum*: depth 365.80 m b.s.f., slide \varnothing 2', EFC O54, MC 53.5 \times 102.6. (J) *Operculodinium microtriatinum*: depth 624.80 m b.s.f., slide \varnothing 1/4', EFC M32, MC 32 \times 103.5; polar view. (K) *Operculodinium xanthium*: depth 365.80 m b.s.f., slide \varnothing 1/4', EFC N48/3, MC 47.2 \times 102.6. (L) *Pentadinium imaginatum*: depth 701.40 m b.s.f., slide \varnothing 1/4', EFC M41, MC 40.5 \times 103.2; polar view. (M) *Pentadinium laticinctum*: depth 502.90 m b.s.f., slide \varnothing 1/4', EFC L33/1, MC 32.8 \times 104.4. (N) *Pentadinium lophophorum*: depth 472.40 m b.s.f., slide \varnothing 1/4', EFC P33/3, MC 32.5 \times 100.5; oblique polar view.

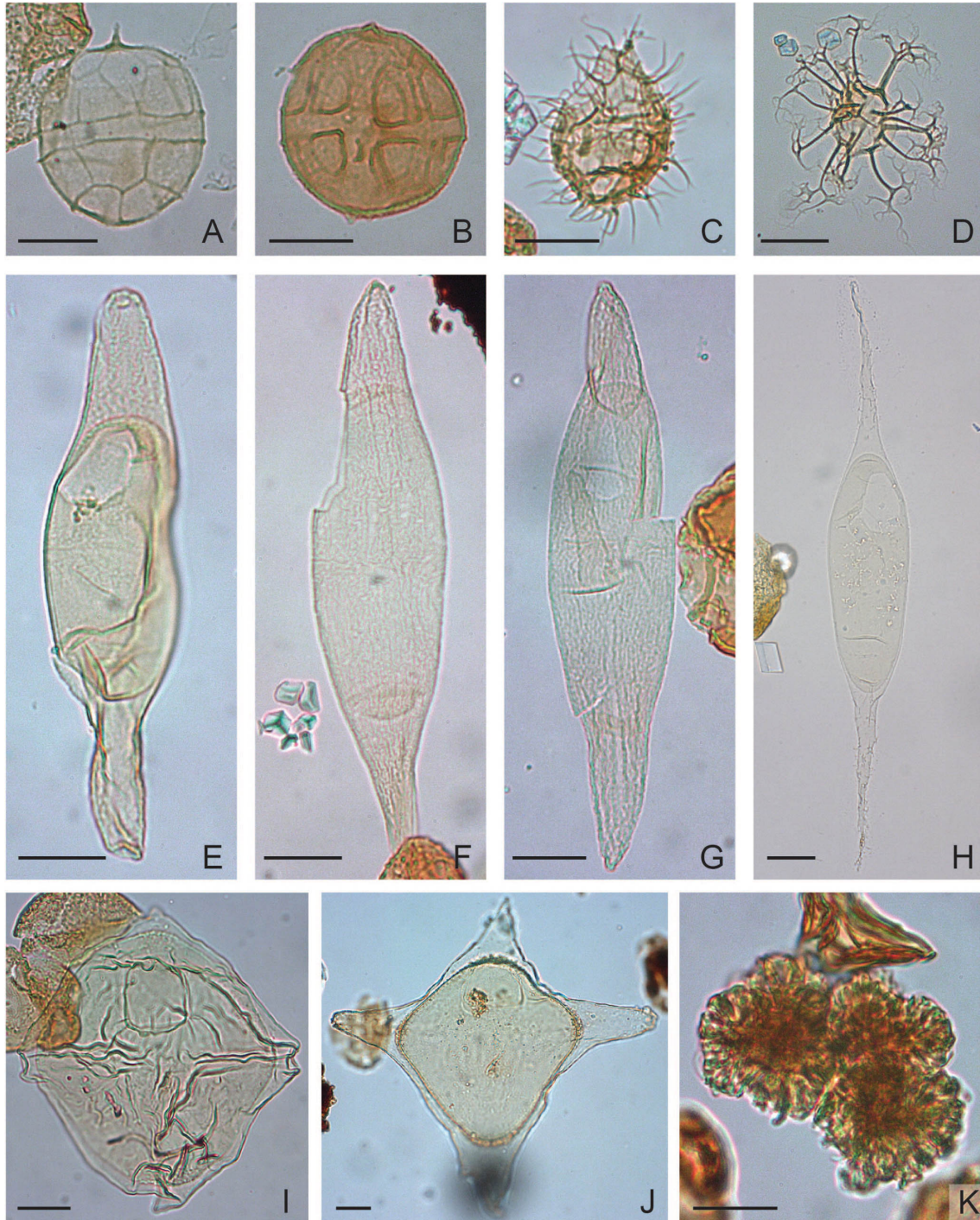


Plate 6. (A) *Phthanoperidinium amoenum*: depth 670.60 m b.s.f., slide \varnothing 1/4', EFC L60/1, MC 59 \times 105. (B) *Phthanoperidinium geminatum*: depth 853.40 m b.s.f., slide \varnothing 1/4', EFC M29/3, MC 29 \times 103. (C) *Phthanoperidinium comatum*: depth 792.50 m b.s.f., slide \varnothing 1/4', EFC L37/4, MC 37 \times 104.5; oblique right lateral view. (D) *Reticulosphaera actinocoronata*: depth 823.00 m b.s.f., slide \varnothing 1/4', EFC M37/1, MC 36.9 \times 104. (E) *Svalbardella cooksoniae*: depth 853.40 m b.s.f., slide \varnothing 1/4', EFC N34/2, MC 34 \times 103; oblique right lateral view. (F) *Svalbardella cooksoniae*: depth 502.90 m b.s.f., slide \varnothing 1/4', EFC T63/3, MC 61.5 \times 96.8; right lateral view. (G) *Svalbardella cooksoniae*: depth 472.40 m b.s.f., slide \varnothing 1/4', EFC Q59/3, MC 58.5 \times 99.5. (H) *Palaeocystodinium teespinosum*: depth 701.40 m b.s.f., slide \varnothing 1/4', EFC W38/1, MC 37.5 \times 94.3. (I) *Rhombodinium draco*: depth 548.60 m b.s.f., slide \varnothing 1/4', EFC L41/2, MC 41 \times 105. (J) *Rhombodinium?* *longimanum*: depth 365.80 m b.s.f., slide \varnothing 2', EFC H38/4, MC 38 \times 107.3. (K) *Botryococcus* spp: depth 670.6 m b.s.f., slide \varnothing 1/4', EFC L49/4, MC 48.7 \times 104.5.

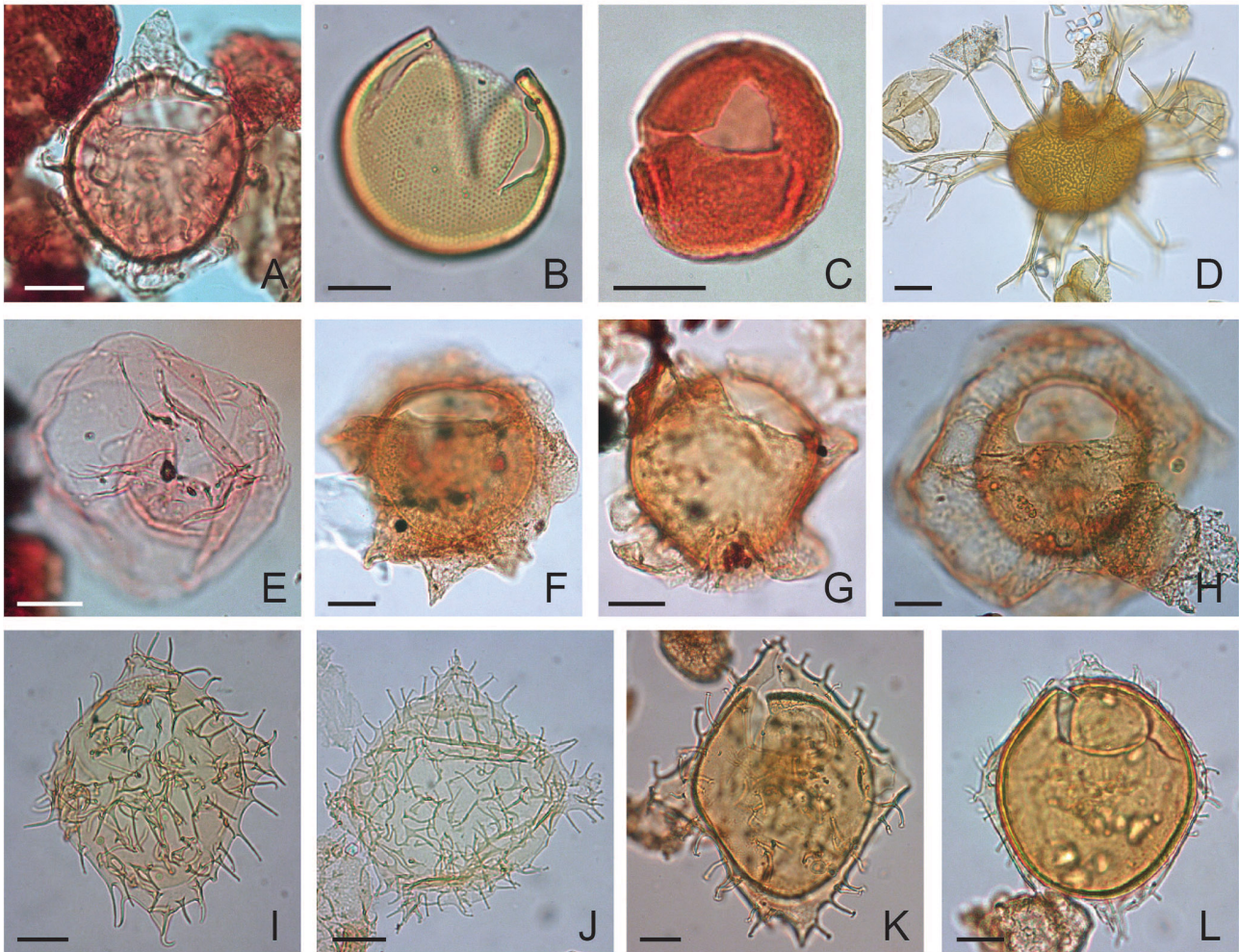


Plate 7. (A) *Samlandia chlamydophora*: depth 1005.84 m b.s.f., slide K-181, F-3, EFC O49/1, MC 48.3 × 102. (B) *Tasmanites* spp.: depth 670.60 m b.s.f., slide Ø 1/4', EFC M62/4, MC 61.4 × 104. (C) *Tectatodinium pellitum*: depth 1036.32 m b.s.f., slide K-180, F-2, EFC J44, MC 43.4 × 107. (D) *Spiniferites manumii*: depth 624.80 m b.s.f., slide Ø 1/4', EFC F36/4, MC 36.2 × 109.4. (E) *Thalassiphora delicata*: depth 1036.32 m b.s.f., slide K-180, F-2, EFC P45, MC 44.5 × 100.7; oblique left lateral view. (F) The specimens resemble morphotype A (Pross, 2001b) of *Thalassiphora pelagica*: depth 487.70 m b.s.f., slide Ø 2', EFC R35/3, MC 35 × 98.5. (G) The specimens resemble morphotype A of *Thalassiphora pelagica*: depth 502.90 m b.s.f., slide Ø 1/4', EFC Q56/4, MC 56 × 99.7. (H) *Thalassiphora pelagica*: depth 365.80 m b.s.f., slide Ø 2', EFC O58, MC 57 × 101.7. (I) *Wetzeliella symmetrica*: depth 457.20 m b.s.f., slide Ø 1/4', EFC L49/2, MC 49.1 × 105. (J) *Wetzeliella gochtii*: depth 609.70 m b.s.f., slide Ø 1/4', EFC L49/3, MC 48 × 104.5. (K) *Wetzeliella articulata*: depth 365.80 m b.s.f., slide Ø 2', EFC M37/1, MC 36.5 × 104.1. (L) *Dracodinium eoceanicum*: depth 823.00 m b.s.f., slide Ø 1/4', EFC M51/3, MC 50.4 × 103.5.

nise FOs. Furthermore, the key age markers for some of the zonal–subzonal division were not recorded (e.g. *Artemisiocysta cladodichotoma*, *Thalassiphora reticulata* and *Saturnodinium pansum*). Therefore, not all the zonal–subzonal boundaries in the well 11/10-1 could be determined with confidence. The dinocyst zonal subdivision of the 11/10-1 well is shown in Fig. 3. *Eatonicysta ursulae*, *Cerodinium depressum* and *Thalassiphora delicata* occur in the lowermost studied sample at 1036.32 m b.s.f. (Fig. 3). In Germany, the LOs of *Cerodinium depressum* and *Thalassiphora delicata* mark the top of the D9nb subzone, while the LO of *Eatonicysta ursu-*

lae marks the top of the D9na subzone (Köthe, 1990; Köthe and Piesker, 2007). Also, the LO of *Eatonicysta ursulae* is an important earliest Lutetian marker in the western North Sea basin (Bujak and Mudge, 1994) and the Norwegian–Greenland Sea (Eldrett et al., 2004). Based on the above, the sample at 1036.32 m b.s.f. is assigned to the D9na subzone and thus of earliest Lutetian age.

The top of the NSO-1 zone and the D12nc subzone is defined by the highest occurrence of *A. diktyoplokum* and is thus placed at 883.90 m b.s.f. The Eocene–Oligocene dinocyst assemblages therefore suggest that the middle

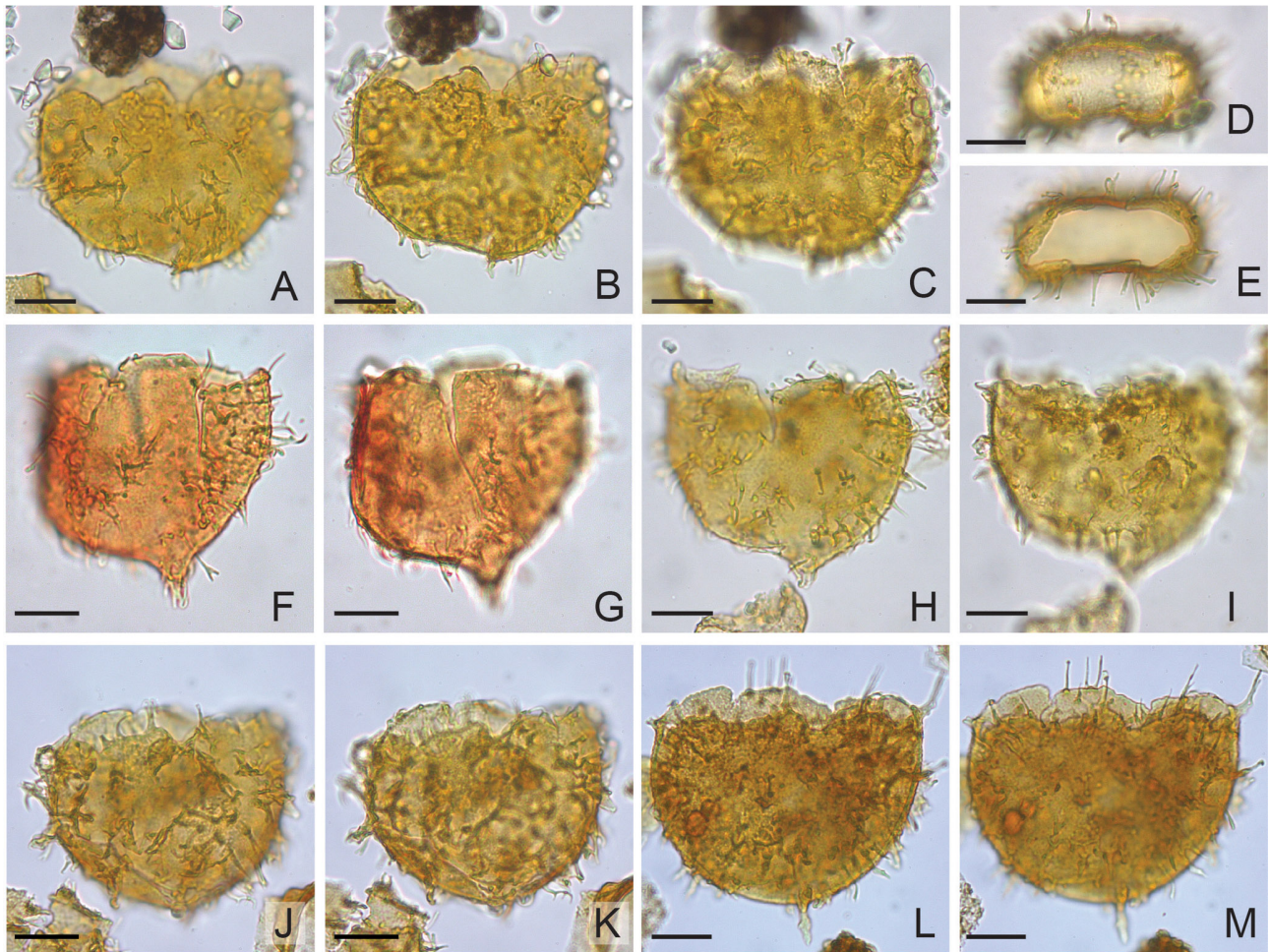


Plate 8. (A) *Areoligera? barskii* sp. nov. holotype: depth 533.40 m b.s.f. or 1750 ft, slide \varnothing 1/4', EFC O26, MC 26 \times 102, ventral surface. (B) The same specimen, central part. (C) The same specimen, dorsal surface. (D) *Areoligera? barskii* sp. nov.: depth 640.1 m b.s.f. or 2100 ft, slide \varnothing 1/4', EFC N23/1, MC 23 \times 103, antapex in polar view. (E) The same specimen, apex in polar view, without operculum. (F) *Areoligera? barskii* sp. nov. Paratype: depth 533.40 m b.s.f. or 1750 ft, slide \varnothing 1/4', EFC M32/1, MC 32 \times 104, ventral surface. (G) The same specimen, dorsal surface. (H) *Areoligera? barskii* sp. nov. Paratype: depth 640.1 m b.s.f. or 2010 ft, slide \varnothing 1/4', EFC S60/1, MC 59.2 \times 98.4, ventral surface. (I) The same specimen, dorsal surface. (J) *Areoligera? barskii* sp. nov.: depth 533.40 m b.s.f. or 1750 ft, slide \varnothing 1/4', EFC R58/1, MC 56.8 \times 99.2, ventral surface. (K) The same specimen, dorsal surface. (L) *Areoligera? barskii* sp. nov.: depth 533.40 m b.s.f. or 1750 ft, slide \varnothing 1/4', EFC L35, MC 34.8 \times 104.5, ventral surface. (M) The same specimen, dorsal surface.

Lutetian–Priabonian strata covering the D9nb to D12nb sub-zones are either condensed or missing (Fig. 2), which is in agreement with the local lithostratigraphical model (Eidvin et al., 2014). This hiatus spanning the middle to late Eocene is estimated to represent at least 13 Myr.

Glaphrocysta semitecta has its LO in the uppermost part of the NSO-2 zone (cf. Van Simaey et al., 2005b). In the 11/10-1 well, the top of the persistent occurrence of the species is at 823.00 m b.s.f., which suggests the presence of the NSO-2 zone. The FO of *Chiroptidium galea* defines the base of the D14na subzone and the base of the NSO-3 zone. This event was tentatively positioned at 762.00 m b.s.f. by Śliwińska and Heilmann-Clausen (2011). In this study the last common occurrence of this species (>4% of the total

dinocyst assemblage) is at 762.00 m b.s.f., and the base of D14na and NSO-3 is thus tentatively placed at this depth (Fig. 3).

The LO of *Phthanoperidinium comatum* marks the top of the NSO-3 zone at 563.90 m b.s.f. (Van Simaey et al., 2005b) and the upper part of the D14na subzone (cf. Köthe and Piesker, 2007; Figs. 3, 7). An intrazonal event for the NSO-3 zone (cf. Van Simaey et al., 2005b) in the 11/10-1 well is the presence of *Spiniferites manumii*, which was observed between 671.0 and 610.0 m b.s.f. (Fig. 3).

The hiatus (or condensed interval) at the Rupelian–Chattian boundary found at, or close to, 411.50 m b.s.f. is equivalent to the duration of the D14nb subzone of Köthe (1990, 2005) and the NSO-5 zone (and possibly also

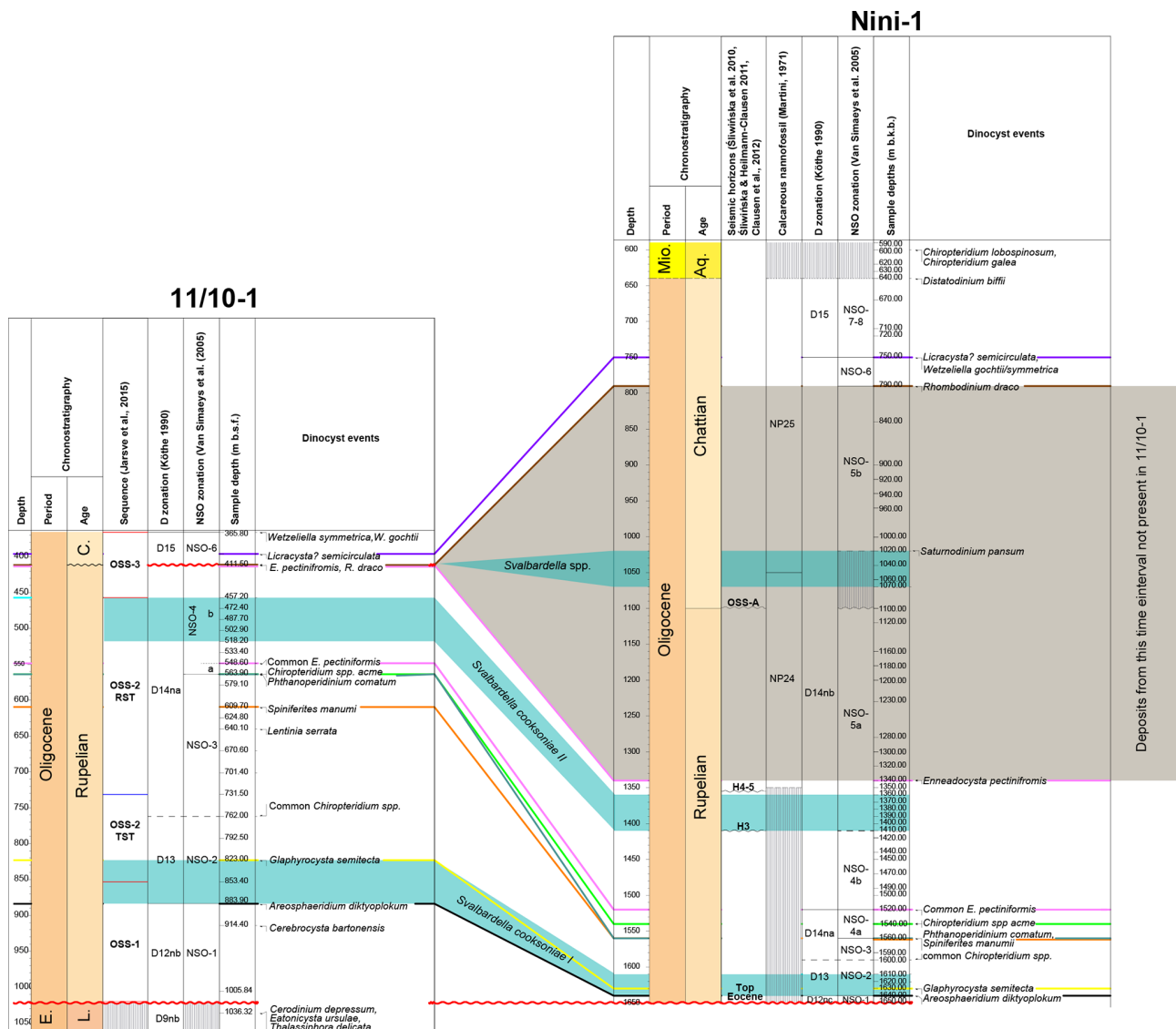


Figure 6. Correlation between the 11/10-1 and the Nini-1 well. Nini-1: distribution of the NP zones after Śliwińska et al. (2014); dinocyst events after Śliwińska (2009), Śliwińska et al. (2010), Śliwińska and Heilmann-Clausen (2011), and Clausen et al. (2012); and the key seismic sequences and surfaces after Śliwińska et al. (2010) and Clausen et al. (2012). C. – Chattian. E. – Eocene. L. – Lutetian. Mio. – Miocene. Aq. – Aquitanian.

the NSO-4b subzone) of Van Simaey et al. (2005b). These zones and subzones span the interval between the LO of *Enneadocysta pectiniformis* (the last common occurrence of *E. pectiniformis* occurs at the top of the NSO-4a subzone, and the LO occurs at the top of the D14na subzone; Fig. 7) and the LO of *Rhombodinium draco* (the top of NSO-5b and D14nb subzones; Fig. 7; Köthe, 2005, 1990; Śliwińska et al., 2012; Van Simaey et al., 2005b). In the 11/10-1 well, these two events occur in the same sample (at 411.50 m b.s.f.), suggesting the presence of a hiatus or a condensed section close to this depth. An approximate duration for the hiatus covers the NP23 zone and part of NP24 zone (cf. Van Simaey et al., 2005b) and can thus be estimated to be about 3.5 Myr.

The timing and the duration of the hiatus does not seem to be supported by the existing strontium isotope ages (Fig. 2). However, each of the two strontium-derived ages in the sample above the inferred hiatus or condensed section is based only on a single mollusc fragment. It is possible that one of the fragments collected for strontium isotope analysis might have been reworked.

The uppermost sample analysed at 365.80 m b.s.f. yields *Wetzeliella symmetrica*, while the LO of *Licracysta? semicirculata* is observed in the sample below (396.20 m b.s.f.). In the NSO zonation, the LOs of these two taxa mark the top of the NSO-6 zone (Van Simaey et al., 2005b). The two

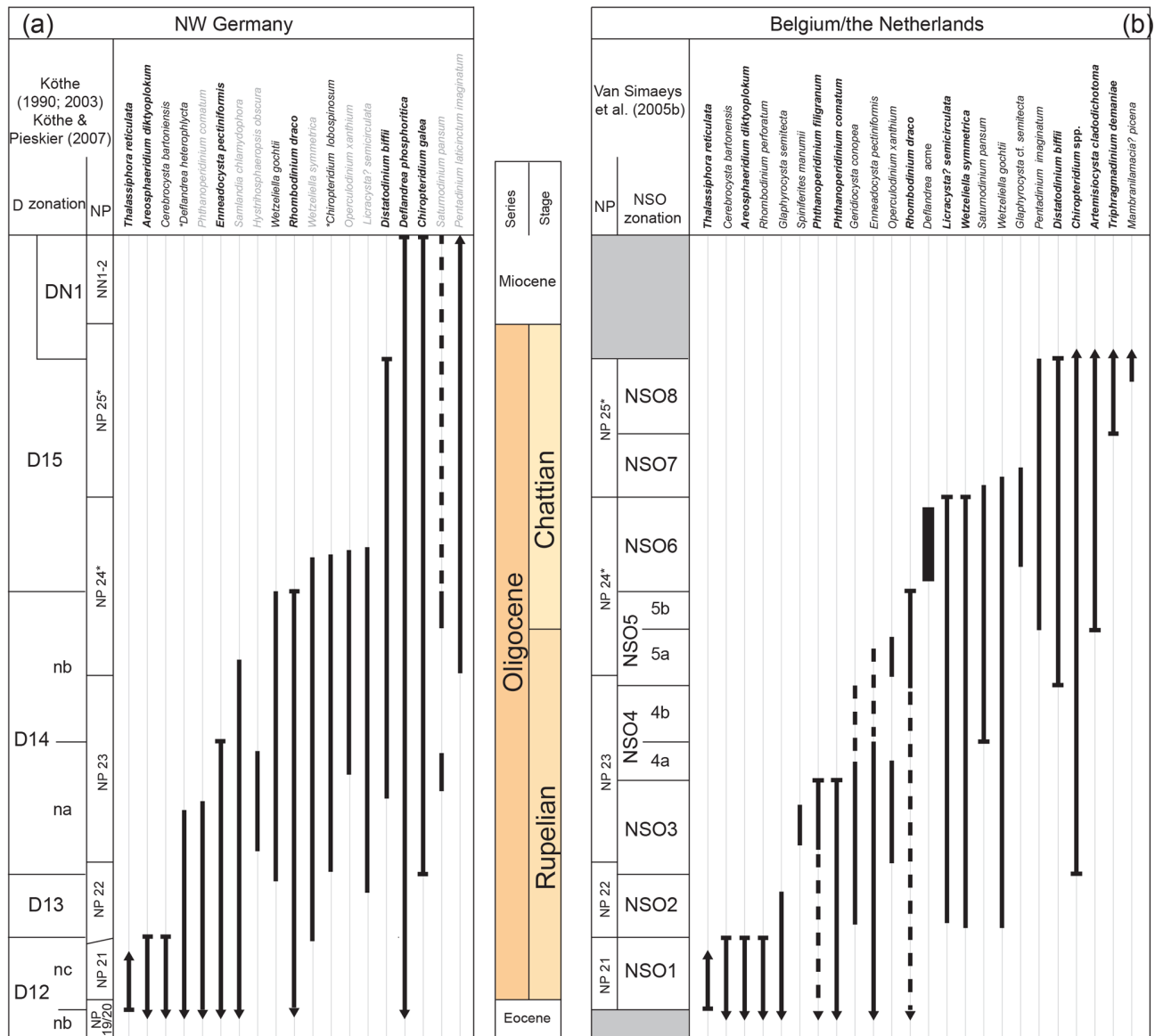


Figure 7. Dinoflagellate zonations used in the present study. Figure modified from Śliwińska et al. (2012). **(a)** The D zonation (Köthe 1990, 2003; Köthe and Piesker, 2007): bold italics – index marker of Köthe (2003), italics – additional marker proposed by Köthe (2003), grey – further species introduced by Köthe and Piesker (2007), * – range of an additional marker modified by Köthe and Piesker (2007). **(b)** The NSO zonation of Van Simaëys et al. (2005b): bold italics – index marker, italics – additional marker. The original calibrations with calcareous nannofossil zonation are shown for each zonation. Because of the use of substitute markers for defining the base of NP24 and NP25, these two zones in northwestern Germany, Belgium and the Netherlands are marked with an asterisk.

uppermost samples are therefore referred to the NSO-6 zone (Fig. 3).

5.2 Palaeoenvironmental changes

Although these analyses were performed on ditch cutting samples and caving may bias some of the results, the trends in relative abundances of the selected dinocyst environmental groups (Table 2) are considered to reflect palaeoenvironmental changes.

5.2.1 Distal–proximal setting and productivity maxima

During deposition of the OSS-1 sequences, the 11/10-1 well was located basinwards of the clinofold break and thus was located in a distal, open marine setting. The clinofolds prograded basinwards during the OSS-2 TST, and the depositional setting of the site thus became more proximal. This part of OSS-2 represents shallow marine shelf deposits (Jarsve et al., 2015). The trend is reflected in dinocyst assemblages, with the typical oceanic taxon *Impagidinium* be-

Table 2. Palaeoecological affinities of the selected dinocyst species and complexes discussed in the study.

Name of the complex and/or taxon	Included genera and/or taxa	Environment
<i>Svalbardella cooksoniae</i>	<i>Svalbardella cooksoniae</i>	Cold surface waters (Head and Norris, 1989; Van Simaey et al., 2005a).
<i>Impagidinium</i> spp.	<i>Impagidinium</i> spp.	Oceanic (Dale, 1996; Wall et al., 1977).
<i>Spiniferites</i>	<i>Spiniferites</i> spp., <i>Achomosphaera</i> spp.	Deep or offshore (Köthe, 1990), inner to outer neritic (Brinkhuis, 1994).
<i>Areoligera</i>	<i>Areoligera</i> spp., <i>Licracysta</i> spp., <i>Chiropteridium</i> spp., <i>Glaphyrocysta</i> spp., <i>Membranophoridium</i> spp.	<i>Areoligera</i> spp. and <i>Glaphyrocysta</i> spp. are considered indicative of deep or offshore waters (Köthe, 1990) or marginal marine to inner neritic (Brinkhuis, 1994). The <i>Areoligera</i> group is equivalent to the “ <i>Chiropteridium</i> + allied types group” sensu Stover and Hardenbol, (1994).
<i>Cleistosphaeridium</i>	<i>Cleistosphaeridium</i> spp., <i>Dapsilidinium</i> spp., <i>Enneadocysta</i> spp., <i>Hystriochokolpoma</i> spp.	Inner to outer neritic (Brinkhuis, 1994).
<i>Thalassiphora</i> spp.	Mainly <i>Thalassiphora pelagica</i>	Tolerant to euxinic conditions (Köthe, 1990), increased nutrient availability and/or low-oxygen conditions (Pross and Schmiedl, 2002).
<i>Homotryblium</i> spp.	Mainly <i>Homotryblium tenuispinosum</i>	Restricted marine, lagoonal (Brinkhuis, 1994).
<i>Deflandrea</i> spp.	<i>Deflandrea</i> spp.	Tolerant of reduced salinity (Köthe, 1990); elevated amounts may be related to pulses of shelf-stored nutrients into the photic zone (Brinkhuis, 1994), and high abundances may be related to possibly brackish, eutrophic setting and/or deltaic settings (Röhl et al., 2013).
<i>Phthanoperidinium</i> spp.	Mainly <i>Phthanoperidinium comatum</i>	Tolerant of reduced or increased salinity (Köthe, 1990); however Barke et al. (2011) found high abundances of <i>Phthanoperidinium</i> spp. (notably mainly <i>P. stockmansii</i>) related to fluxes of freshwater <i>Azolla</i> spores.
<i>Wetzeliiella</i> spp.	<i>Wetzeliiella</i> spp.	Tolerant of reduced salinity (Köthe, 1990); possibly estuarine (Downie et al., 1971), well-mixed and nutrient-rich (see discussion in Sluijs et al., 2005) neritic waters (Brinkhuis, 1994).

ing restricted to the lower part of the succession (Fig. 5), i.e. below the maximum flooding surface (mfs) at 730 m b.s.f. When present, the genus is rare (i.e. less than two specimens in the entire slide), but apparently, even such low abundances may indicate the influence of oceanic, open marine waters (Wall et al., 1977). The succession below the maximum flooding surface is also characterised by abundance maxima of *Spiniferites* and *Areoligera* (Fig. 5), thus also suggesting an open marine, distal setting (e.g. Brinkhuis, 1994; Table 2). The internal architecture of OSS-2 RST suggests that this tract of the sequence was deposited in a proximal setting of a fluvio-deltaic regime (Jarsve et al., 2015). This interval con-

sists of coarse-grained deposits, representing shifting deltaic lobes, that prograded basinwards (towards the south to southwest). The distribution of the dinocysts within this sequence is profoundly different (Fig. 6). A proximal, high nutrient setting in well-mixed waters is implied by the highest concentration of peridinioid cysts: the two abundance peaks of *Wetzeliiella* spp. and local maxima of *Deflandrea* spp. (Downie et al., 1971; Köthe, 1990). High nutrient fluxes, corresponding to the productivity maxima (Fig. 5) and caused by abundance maxima of peridinioid cysts, might have been brought in by a nearby river. Typical lagoonal dinocysts, *Homotryblium* spp., also have their maximum abundances within OSS-2 RST, al-

beit not forming more than 15 % of the total dinocyst assemblage. The presence of *Homotryblium* spp. may either suggest that lower-salinity waters reached the site or that the *Homotryblium* spp. cysts were transported from lagoons located closer to land. The peak in the relative abundance of *Thalassiphora* spp. may suggest an episode of temporary stratified, oxygen-depleted waters. Furthermore, pronounced changes within the peridinioid cyst assemblages suggest that the environment was highly dynamic; this is expressed by the high abundances of *Wetzeliella*, which do not equate to the pulses of the *Cleistosphaeridium* group.

In contrast to the two other peridinioid groups, *Wetzeliella* spp. and *Deflandrea* spp., the *Phthanoperidinium* group is most common in OSS-1 and OSS-2 TST. Low abundances of *Phthanoperidinium* within OSS-2 RST may reflect the fact that *Phthanoperidinium comatum* (the main taxon within the group; see Table 2 and Fig. 4) has its LO in the middle part of the sequence. It is, however, possible that *Phthanoperidinium* preferred slightly deeper and/or lower-salinity waters. The similarity in the abundance trends of *Wetzeliella* spp. and *Deflandrea* spp. (Fig. 5) suggests that these groups have fairly similar environmental preferences.

As implied by the seismic study of Jarsve et al. (2015), OSS-3 was most probably deposited in inner-neritic, shallow marine settings. During the deposition of OSS-3, the area around the 11/10-1 well was located landwards of the clinoform break. The three samples available from this sequence have clearly different distributions of dinocysts compared with the sequence below (Fig. 5). The relative decrease (in contrast to OSS-2 RST) in abundance of *Wetzeliella* spp. coincides with high relative abundances of the *Spiniferites*, *Areligera* and *Cleistosphaeridium* environmental groups. This change is linked to lower nutrient availability (there are no deltaic deposits recognised within this succession; cf. Jarsve et al., 2015) and not with the increase in the sea level.

5.2.2 Cold water pulses

Taxa that are typically considered as warm-water indicators, *Lingulodinium machaerophorum* (Marret and Zonneveld, 2003), *Polysphaeridium zoharyi* (Head and Norris, 1989; Marret and Zonneveld, 2003) and *Tectatodinium pellitum* (Head, 1994; cited in Jaramillo and Oboh-Ikuenobe, 1999; Marret and Zonneveld, 2003), are absent to rare in the 11/10-1 well ($\leq 4\%$ of the total dinocyst assemblage; Fig. 4). The relative abundance of these taxa is, however, only slightly lower than in the Eocene sequences (Heilmann-Clausen and Van Simaey, 2005), which were deposited under much warmer sea-surface temperatures (Śliwińska et al., 2019). Furthermore, these warm-water taxa do not show any trends in the data presented here. This is in contrast to *Svalbardella cooksoniae*, which appears in the intervals that can be correlated with the Oligocene cooling events (i.e. the Oi events; Figs. 4–6).

Based on the first stratigraphic occurrence and the distribution of the dinocyst genus *Svalbardella* in the North Atlantic region, Head and Norris (1989) suggested that the taxon is related to cold-water conditions. Subsequently, Van Simaey et al. (2005a) recognised a distinctive, globally distributed *Svalbardella* spp. interval corresponding to the strongest Oligocene glaciation, the Oi-2b cooling event occurring during Chron C9n (earliest Chattian). This was followed by the discovery of a distinctive early Rupelian *Svalbardella cooksoniae* interval correlating with the Oi-1a cooling event (Śliwińska and Heilmann-Clausen, 2011) and a late Rupelian *S. cooksoniae* interval correlating with the Oi-2 cooling event (Clausen et al., 2012). However, while *S. cooksoniae* appeared in various basins in the middle and high northern latitudes during the Oi-1a event, the *S. cooksoniae* interval related to the Oi-2 event has so far only been recognised in one well in the North Sea basin (the Nini-1 well; Clausen et al., 2012). In the 11/10-1 well, two *Svalbardella cooksoniae* intervals were observed. The older interval (top at 823.00 m b.s.f.; marked here as *Svalbardella cooksoniae* I; Figs. 2 and 6) was recognised for the first time by Śliwińska and Heilmann-Clausen (2011) and linked with the Oi-1a cooling event. The younger interval (top at 457.20 m b.s.f., marked here as *Svalbardella cooksoniae* II; Fig. 2) is reported here for the first time.

The early Rupelian *Svalbardella cooksoniae* I interval frames the sequence boundary which corresponds to an erosional surface at the top of the regressive system tract of sequence OSS-1 sensu Jarsve et al. (2015; Fig. 2). Strontium isotope data (Jarsve et al., 2015) collected from the interval where the *Svalbardella cooksoniae* I interval occurs, imply an age of 32.66 Ma for the event. These observations confirm the suggestion of Śliwińska and Heilmann-Clausen (2011) that the earliest Rupelian *S. cooksoniae* interval in the Tethys (Van Mourik and Brinkhuis, 2005), central Europe (Gedl, 2004), the North Sea basin (Schiøler, 2005) and the Norwegian–Greenlandic Sea (Eldrett et al., 2004) is synchronous with the Oi-1a cooling event and coincides with a major eustatic sea-level fall.

The top of the younger *Svalbardella cooksoniae* II interval occurs at 457.20 m b.s.f. (Figs. 2, 4 and 6). The interval is bracketed by the LOs of *Enneadocysta pectiniformis* and *Phthanoperidinium comatum* and is thus of latest Rupelian age. The top of the *S. cooksoniae* II interval also correlates with an erosional surface with deep incisions (the top of the local seismic sequence OSS-2; Jarsve et al., 2015; Figs. 2 and 3). These channel incisions are more severe than those at the top of OSS-1 (at OSS-1 they may be below seismic resolution; see Jarsve et al., 2015). The erosional surface at the top of OSS-2 was interpreted to be of subaerial or shallow marine origin (Jarsve et al., 2015). These observations suggest that the *S. cooksoniae* II interval and the erosional surface are also related to a glacioeustatic sea-level fall, which may have been even larger than the sea-level fall related to the Oi-1a cooling event. However, the precise magnitude of the sea-level drop

associated with these cooling events in the North Sea basin remains uncertain.

The stratigraphic position of the *Svalbardella cooksoniae* II interval (Figs. 2, 3 and 6) in the 11/10-1 well implies that the interval is time equivalent to the *Svalbardella cooksoniae* interval recognised previously in the Nini-1 well by Clausen et al. (2012; Fig. 6). In the Nini-1 well the late Rupelian *S. cooksoniae* interval was observed within a forced regressive unit caused by a climatically induced sea-level fall (Clausen et al., 2012). These authors deduced that the presence of *Svalbardella* was related to one of the late Rupelian glacial events (most probably Oi-2 sensu Pekar et al., 2002). Strontium isotope data from the 11/10-1 well imply an age of 30.11 Ma for this depth (Jarsve et al., 2015) and thus support this interpretation (Fig. 2). The improved age model may furthermore imply that the two middle Oligocene cooling events (Oi-2a dated as ~ 28 Ma – Chron C9r – and Oi-2b dated as ~ 27 Ma – Chron C9n) fall within the hiatus at the Rupelian–Chattian boundary (Fig. 2), which in the 11/10-1 well is around 411.5 m b.s.f. Close to this depth, a horizon with rock fragments or pebbles (NPD_report, 1969b) and abundant molluscs and mollusc fragments (Eidvin et al., 2013) was identified. This horizon is similar to the gravel layer from the eastern North Sea basin, which marks the sequence boundary at the Oligocene–Miocene boundary (Rasmussen et al., 2010), and the pebble layer in well 11/10-1 can be interpreted as an indicator of the unconformity. Even though the horizon is not mapped as a sequence boundary in the sequence stratigraphic interpretation of Jarsve et al. (2015; i.e. it is located within OSS-3), Jarsve et al. (2015) observed that in the vicinity of the 11/10-1 well this sequence consists of parallel subhorizontal reflectors interpreted to indicate deposition in a shallow marine environment. The base of sequence OSS-3 (close to 457 m b.s.f.) is characterised by fluvial incisions, while the top of the sequence (close to 366 m b.s.f.) is interpreted as a subaerial unconformity (Jarsve et al., 2015): the entire sequence consists of sandy deposits (Jarsve et al., 2015; NPD_report, 1969a). It is possible that the area within the vicinity of the 11/10-1 well acted as a bypass zone or that erosion and/or non-deposition took place within OSS-3 (Jarsve et al., 2015). Thus, the hiatus related to the Rupelian–Chattian boundary may be indistinguishable from other horizons observed within the sequence.

Based on biostratigraphic correlation with the Nini-1 well (Fig. 4) and the stratigraphic studies of the North Sea basin by Schiøler et al. (2007), it seems that the hiatus at the Rupelian–Chattian boundary in the 11/10-1 well covers the time span during which the thick middle Oligocene sediment package located in more distal settings (i.e. in the area of the Nini-1 well) was deposited, including the *Svalbardella* interval related to the Oi-2b cooling. The correlation between the two wells does not support the suggestion of Jarsve et al. (2015) that the local sequence OSS-4 is related to the Oi-2b cooling phase but rather with one of the younger cooling events.

6 Conclusions

Even though this study of the dinocysts from the Syracuse Oils Norge A/S 11/10-1 well is based exclusively on ditch cuttings, limiting age control to LOs, the rich, diverse and well-preserved dinocyst assemblages are excellent for stratigraphic correlation and palaeoenvironmental determinations. The LOs of *Phthanoperidinium comatum*, *Spiniferites manumii* and *Lentinia serrata* seem to be reliable, synchronous markers for Rupelian stratigraphy not only within the North Sea basin but also across the North Atlantic. This study also confirms that the LO of *Glaphyrocysta semitecta* is synchronous within the eastern North Sea basin and Tethys. The LOs of *Enneadocysta pectiniformis* and *Rhodobinium draco* can also be applied for inter-basinal stratigraphy, even though the events have a known, moderate diachroneity between the basins. One of the most significant findings is that the LO of *Areosphaeridium diktyoplokum* is about 130 m above the top Eocene horizon (equivalent to the Eocene–Oligocene boundary), which indicates that the lowermost Rupelian succession in particular is exceptionally thick. The dinocyst assemblages also reveals novel details on the Eocene–Oligocene boundary and the Rupelian–Chattian boundary. These assemblages suggest that the middle–upper Lutetian–Priabonian deposits are missing (indicating a hiatus covering ~ 13 Myr) or are very condensed. Furthermore, dinocyst stratigraphy reveals a hiatus or condensed interval spanning ~ 3.5 Myr at the Rupelian–Chattian boundary.

The distribution of selected dinocyst environmental groups has also been analysed within the regional stratigraphic sequence framework. The groups seem to be good indicators of depositional changes. For example, dinocyst assemblages within OSS-1 are dominated by *Spiniferites* and *Areoligera* groups and characterised by the presence of *Impagidinium* spp. This confirms that the sequence was deposited in the most distal, deep and outer-neritic setting of the basin. In contrast, the inner-neritic, deltaic setting of OSS-2 RST is reflected by high counts of *Wetzeliella* spp. and *Deflandrea* spp. interfingering with maximum abundances of the *Cleistosphaeridium* group. This is interpreted as to reflect high nutrient pulses (related to the high values of $P/P + G$) carried into the basin by rivers and a dynamic, high-energy environment, which is characteristic of deltaic depositional settings. My study indicates a strong climatological imprint on the development of the sequences in the North Sea basin during the Oligocene. The two *Svalbardella cooksoniae* intervals reported in the 11/10-1 well are related to erosional surfaces (sequence boundaries), apparently reflecting glacioeustatic sea-level fall. Both intervals correlate with cooling events, Oi-1a (Śliwińska and Heilmann-Clausen, 2011) and Oi-2 (Clausen et al., 2012; this study), previously defined in the North Sea basin. In conclusion it is postulated that the possible hiatus at the Rupelian–Chattian boundary covers the time span comprising two middle Oligocene cooling events (Oi-2a and Oi-2b).

7 Dinocyst taxonomy: formal description of new taxon

Systematic palaeontology

Division Dinoflagellata (Bütschli 1885) Fensome et al., 1993

Subdivision Dinokaryota Fensome et al., 1993

Class Dinophyceae Pascher 1914

Subclass Peridiniphyceae Fensome et al. 1993

Order Gonyaulacales Taylor 1980

Suborder Gonyaulacineae

Family Areoligeraceae Evitt, 1963

Genus *Areoligera* Lejeune-Carpentier, 1938

Species *Areoligera? barskii* sp. nov. (Plate 8).

Derivation of name

Named after palaeontologist Marcin Barski (Warsaw University), who introduced me to dinocysts and was my BSc supervisor.

Diagnosis

A species of *Areoligera* with proximochorate ornamentation. The surface of the cyst is smooth or microreticulate. The dorsoventral outline is subspherical, often asymmetrical and usually more pronounced on the left side. Intratabular or nontabular processes are distally free, sometimes connected basally. Processes are tapering often of various length but are generally not longer than 12 µm and are distally capitate but can also be bifurcate, acuminate, oblate and digitate. The sulcal area and the central part of the antapical plate (1''''') are free from ornamentation. Except for the archeopyle margin, there is no tabulation on the ventral surface.

Holotype

Well 11/10-1, depth 533.40 m b.s.f. or 1750 ft b.s.f., slide Ø 1/4'; England Finder Coordinates (EFCs) O26 (Plate 8A–C). Palynological slides are stored at the Norwegian Petroleum Directorate in Stavanger, Norway.

Paratype

Well 11/10-1, depth 533.40 m b.s.f. or 1750 ft, slide Ø 1/4', EFC M32/1 (Plate 8F, G); depth 640.10 m b.s.f. or 2100 ft b.s.f., slide Ø 1/4', EFC S60/1 (Plate 8H, I). Palynological slides are stored at the Norwegian Petroleum Directorate in Stavanger, Norway.

Material

Ditch cutting samples from an industrial Syracuse Oils Norge A/S well 11/10-1.

Locality and horizon

So far the taxon has only been observed in Rupelian strata in the North Sea basin in well 11/10-1 (the interval between 823 and 412 m b.s.f.).

Age

Rupelian.

Description

The cyst is dorsoventrally flattened, with a convex dorsal side and a concave ventral side (Plate 8D and E). The well-developed sulcal notch is strongly offset to the left (Plate 8A–C). The autophragm can be up to 3 µm thick. On the ventral side the processes are often single but are usually arranged in soleate or arcuate complexes. The sulcal area is devoid of processes. The cingulum from the ventral side appears to be free of processes. The dorsal surface is more densely covered with processes, but their arrangement is not clearly seen. The outline of the cyst is circular (Plate 8L and M) or subcircular, with one or two antapical lobes. Antapex can have either a moderately sized (Plate 8J–K) or pronounced (Plate 8F–I) left antapical lobe or a minute horn (Plate 8J–M). The outline of the central body is similar to other species of *Areoligera*, e.g. *Areoligera campoensis*. The antapical lobe or horn can carry processes (Plate 8F–IL and M). The archeopyle is apical and tetratabular. The operculum is free.

Dimensions

Holotype: 84 × 66 µm ($w \times l$). Paratype: 79 × 62.5 µm ($w \times l$). Average dimensions ($n = 10$): width 77.13 µm (62.50–91 µm), length 63.00 µm (57–69 µm). The length does not include the operculum. The height of the antapical lobe or horn is up to 7.5 µm. Maximum length of processes 12 µm.

Stratigraphic range and occurrence

The LO of *Areoligera? barskii* sp. nov. occurs at 412 m b.s.f., the same depth as the LOs of *Rhombodinium draco* and *Enneadocysta pectiniformis* at 412 m b.s.f. The LO of *A.? barskii* sp. nov. (note that this may not be in situ but may be an effect of caving) is at the same level as the LO of *Glaphyrocysta semitecta* at 823.0 m b.s.f. *Areoligera.? barskii* is rare (< 1 % of the total dinocyst assemblage) to abundant (> 50 % of the total dinocyst assemblage).

Genus assignment

The species is questionably included in the genus *Areoligera*. It differs from *Canningia*, which has an autophragm and an ectophragm and is uniformly ornamented. *Cerbia* is clearly paratabulate, and both mid-dorsal and mid-ventral areas are essentially devoid of ornament. Furthermore, *Cerbia* has usually low lateral projections and clearly defined, significantly shorter processes. *Cyclonephelium* has linear ornamentation, and, like *Chiropteridium*, the ornamentation is reduced or lacking on both mid-ventral and mid-dorsal areas. *Glaphyrocysta* also differs in having distally connected processes.

Remarks

Areoligera? barskii sp. nov. is distinguished from other species of the genus by the length of the processes, which are on average only 15%–20% of the cyst width. The central body outline of *Areoligera? barskii* and the short length of the processes may resemble *Areoligera guembelii*, but processes in *A. guembelii* are only capitate and bifurcate and are arranged in pronounced annulate complexes. Actually, all known species of *Areoligera* are characterised by rather broad processes (process complexes) and rising soleate or arcuate ridges on their dorsal side (Williams and Downie, 1966). Since ridges are not clearly developed in *Areoligera? barskii* sp. nov., the taxon is only questionably assigned to the genus.

Genus *Enneadocysta* Stover and Williams, 1995, emend. Fensome et al., 2007

Species *Enneadocysta magna* Fensome et al., 2007 (Plate 3L and M)

Remarks

Enneadocysta magna is characterised by its large size and slender licrate processes with highly asymmetrical distal extremities (Fensome et al., 2006; Plate 3M). As noted by Fensome et al. (2006) it may appear similar in overall morphology to *Licracysta? semicirculata*, but it has only one process per plate. When Fensome et al. (2006) described *Enneadocysta magna* as a new species, the authors pointed out that some of the specimens in the type material from the western North Atlantic may have complexly branched processes. This results in an illusion of more than one process per plate, and thus the taxon may resemble *Licracysta? semicirculata* (cf. Plate 2.13–16 in Fensome et al., 2006).

In my material some specimens of *Enneadocysta magna* possess broad (precingular) to very broad (postcingular) processes (Plate 3L) and appear to be thicker than in the type material (cf. plate 1.9–16 in Fensome et al., 2006). There is only one process per plate, but the processes resemble processes of *L.? semicirculata* (Plate 3L).

Data availability. Raw dinocyst counts are available upon a written request to the author.

Appendix A: Collecting coordinates for dinocysts

Selected dinocysts are illustrated in Plates 1–8. So that every photographed specimen can be located, I provide England Finder Coordinates (EFCs) in the plate captions. The England Finder has been developed as a tool for easy allocation of specimens on a slide (in, for example, palynological and nanofossil studies) regardless of the type and/or manufacturer of microscope used. However, the England Finder is rather costly, while alternative methods are either damaging to the slide or time-consuming (e.g. Sterrenburg et al., 2012). Relocation of the selected specimen may otherwise be difficult, since the coordinate system for each microscope differs, even for those manufactured by the same company. Therefore, an alternative, time-efficient and cost-free method for refinding palynomorphs is proposed here.

When a palynological slide is placed on the microscope stage (Fig. A1) the upper right corner (here named the A point) will always have the same microscope coordinates (MCs) regardless of the size of the slide. Therefore, the A point can be used as the origin point of a coordinate system for the slide. Knowing the A point of a given microscope, one can convert MCs between microscopes without the use of the England Finder. To obtain the most precise reading, the coordinates of the A point must be taken using a low-magnification objective ($\times 10$). If the upper right corner of the slide is broken or rounded, the location of the A point can be extrapolated using the right upper side of the slide (Fig. A1).

In this study the A point for the microscope utilised (M1) has coordinates 0.4×90.3 ($XM1 \times YM1$); the MCs for each specimen are given in the plate caption ($X1 \times Y1$). For relocating a selected specimen on another microscope (M2), the A point of M2 needs to be measured first ($XM2 \times YM2$). In M1 both Y and X axes increase ($X: 0 \rightarrow 90$; $Y: 90 \rightarrow 135$) away from the A point (Fig. A1). If in M2 the X and Y axes also increase, then the coordinates of the selected specimen under microscope M2 can be calculated as follows:

$$Xs \text{ for M2} = (X1 - XM1) + XM2, \quad (\text{A1})$$

$$Ys \text{ for M2} = (Y1 - YM1) + YM2. \quad (\text{A2})$$

If in M2 the axes decrease, then

$$Xs \text{ for M2} = -((X1 - XM1) - XM2), \quad (\text{A3})$$

$$Ys \text{ for M2} = -((Y1 - YM1) - YM2). \quad (\text{A4})$$

This method is viable under the following conditions:

1. The microscope is equipped with a millimetre scale (horizontal and vertical; X and Y).
2. The millimetre scale is positioned on the microscope stage so that it is possible to take coordinates for the A point.

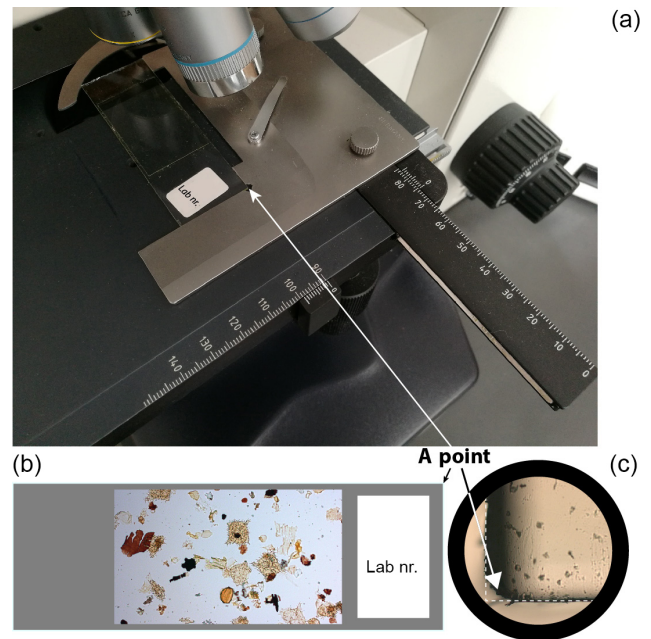


Figure A1. A technique for determining the location of specimens on different microscopes. (a) A typical palynological slide is placed at the microscope stage. The coordinates are taken on the millimetre-scale coordinate system (X is horizontal; Y is vertical). On the depicted microscope the X scale is from 0 to 90 and the Y scale is from 90 to 150. (b) The A point is located in the upper right corner of the slide. (c) The A point of the slide seen under the microscope with $\times 10$ magnification. The corner is (often) rounded, so the precise position of the A point can be extrapolated as shown here. The position of the A point is marked with an arrow. Once the slide is placed properly, the coordinates of the A point can be taken. If all the slides are analysed under the same microscope the A-point coordinates need to be taken only once. Then, slides can be analysed and coordinates of selected specimens can be taken in a traditional manner.

This system of collecting coordinates is more time efficient than collecting coordinates with the England Finder (EF), as switching between the original slide and the EF slide is not needed. Furthermore, once the difference in the coordinates of the A point between two microscopes is known, it is easy to switch between microscopes. As an example, my work microscope has the A-point coordinates 0.4×90.3 , while my microscope at home has the A-point coordinates 100.7×0.6 . So to relocate the specimen at my home microscope, with coordinates taken from my work microscope, I need to add 99.7 on the X axis and subtract 89.7 on the Y axis.

Author contributions. KKŚ designed the research, carried out dinocyst analysis, interpreted the data and wrote the paper.

Competing interests. The authors declare that they have no conflict of interest.

Acknowledgements. This research was funded by the Danish Council for Independent Research – Natural Sciences (DFF/FNU; grant no. 11-107497). Henrik Nøhr-Hansen and Claus Heilmann-Clausen are thanked for their help in identifying some of the reworked taxa. Karen Dybkjær, Henrik Vosgerau and Jon R. Ineson provided valuable comments regarding the final version of the paper. The author acknowledges the Norwegian Petroleum Directorate (NPD) for placing palynological slides at her disposal. Preparation methods for palynological slides prepared by NPD were provided by Robert Williams. Figure 1 was made by Jette Halskov (GEUS). Palynological slides from two samples (K-181 and K-180) were prepared by Kirsten Rosendal (IG, AU) for the author's PhD project, which was funded by Aarhus University. Figures 3–5 were prepared using the StrataBugs v2.0 charts. I thank Francesca Sangiorgi and two reviewers, Graham Williams and Alexander Houben, for their valuable comments and suggestions, which helped to improve this paper.

Financial support. This research has been supported by the Danish Council for Independent Research – Natural Sciences (DFF/FNU; grant no. 11-107497).

Review statement. This paper was edited by Francesca Sangiorgi and reviewed by Alexander Houben and Graham Williams.

References

- Abels, H. A., Van Simaey, S., Hilgen, F. J., De Man, E., and Vandenberghe, N.: Obliquity-dominated glacio-eustatic sea level change in the early Oligocene: Evidence from the shallow marine siliciclastic Rupelian stratotype (Boom Formation, Belgium), *Terra Nov.*, 19, 65–73, <https://doi.org/10.1111/j.1365-3121.2006.00716.x>, 2007.
- Barke, J., Abels, H. A., Sangiorgi, F., Greenwood, D. R., Sweet, A. R., Donders, T., Reichart, G. J., Lotter, A. F., and Brinkhuis, H.: Orbitally forced *Azolla* blooms and Middle Eocene Arctic hydrology: Clues from palynology, *Geology*, 39, 427–430, <https://doi.org/10.1130/G31640.1>, 2011.
- Bartek, L. R., Vail, P. R., Anderson, J. B., Emmet, P. A., and Wu, S.: Effect of Cenozoic ice sheet fluctuations in Antarctica on the stratigraphic signature of the Neogene, *J. Geophys. Res.-Sol. Ea.*, 96, 6753–6778, <https://doi.org/10.1029/90JB02528>, 1991.
- Bijl, P. K., Pross, J., Warnaar, J., Stickley, C. E., Huber, M., Guerstein, R., Houben, A. J. P., Sluijs, A., Visscher, H., and Brinkhuis, H.: Environmental forcings of Paleogene Southern Ocean dinoflagellate biogeography, *Paleoceanography*, 26, PA1202, <https://doi.org/10.1029/2009PA001905>, 2011.
- Bijl, P. K., Brinkhuis, H., Egger, L. M., Eldrett, J. S., Frieling, J., Grothe, A., Houben, A. J. P., Pross, J., Śliwińska, K. K., and Sluijs, A.: Comment on “Wetzeliella and its allies – the “hole” story: a taxonomic revision of the Paleogene dinoflagellate sub-family Wetzelielloideae” by Williams et al. (2015), *Palynology*, 41, 423–429, <https://doi.org/10.1080/01916122.2016.1235056>, 2017.
- Brinkhuis, H.: Late Eocene to Early Oligocene dinoflagellate cysts from the Priabonian type-area (Northeast Italy): biostratigraphy and paleoenvironmental interpretation, *Palaeogeogr. Palaeoclimatol.*, 170, 121–163, [https://doi.org/10.1016/0031-0182\(94\)90168-6](https://doi.org/10.1016/0031-0182(94)90168-6), 1994.
- Bujak, J. and Mudge, D.: A high-resolution North Sea Eocene dinocyst zonation, *J. Geol. Soc. London.*, 151, 449–462, 1994.
- Clausen, O. R., Śliwińska, K. K., and Gołedowski, B.: Oligocene climate changes controlling forced regression in the eastern North Sea, *Mar. Pet. Geol.*, 29, 1–14, <https://doi.org/10.1016/j.marpetgeo.2011.10.002>, 2012.
- Coccioni, R., Montanari, A., Bice, D., Brinkhuis, H., Deino, A., Frontalini, F., Lirer, F., Maiorano, P., Monechi, S., Pross, J., Sagnotti, L., Sideri, M., Sprovieri, M., Tateo, F., Rochette, P., Touchard, Y., Van Simaey, S., and Williams, G. L.: The Global Stratotype Section and Point (GSSP) for the base of the Chattian Stage (Paleogene System, Oligocene Series) at Monte Cagnero, Italy, *Episodes*, 41, 17–32, <https://doi.org/10.18814/epiugs/2018/v41i1/018003>, 2018.
- Costa, L. I. and Manum, S. B.: The description of the interregional zonation of the Paleogene (D1–D15) and Miocene (D16–D20), The northwest European Tertiary Basin – Results of the International Geological Correlation Programme, Project No. 124, in: *Geologisches Jahrbuch A*, edited by: Vinken, R., 321–330, 1988.
- Coxall, H. K., Wilson, P. A., Pälike, H., Lear, C. H., and Backman, J.: Rapid stepwise onset of Antarctic glaciation and deeper calcite compensation in the Pacific Ocean, *Nature*, 433, 53–57, <https://doi.org/10.1038/nature03135>, 2005.
- Dale, B.: Dinoflagellate cyst ecology: modeling and geological applications, in: *Palynology: Principles and Applications*. American Association of Stratigraphic Palynologists Foundation, edited by: Jansonius, J. and McGregor, D. C., Dallas, 1249–1276, 1996.
- Damassa, S. P. and Williams, G. L.: Late Eocene-Oligocene dinoflagellate provincialism in the North Atlantic Ocean, in: *Cenozoic Plants and Climates of the Arctic*. NATO ASI Series (Series I: Global Environmental Change), edited by: Boulter, M. C. and Fisher, H. C., Springer, Berlin, Heidelberg, 73–92, 1994.
- Danielsen, M., Michelsen, O., and Clausen, O. R.: Oligocene sequence stratigraphy and basin development in the Danish North Sea sector based on log interpretations, *Mar. Pet. Geol.*, 14, 931–950, [https://doi.org/10.1016/S0264-8172\(97\)00043-3](https://doi.org/10.1016/S0264-8172(97)00043-3), 1997.
- de Kaenel, E. and Villa, G.: Oligocene-Miocene calcareous nannofossil biostratigraphy and paleoecology from the Iberia Abyssal Plain, *Proc. Ocean Drill. Program. Sci. Results*, 149, 79–145, <https://doi.org/10.2973/odp.proc.sr.149.208.1996>, 1996.
- De Schepper, S., Head, M. J., and Louwye, S.: Pliocene dinoflagellate cyst stratigraphy, palaeoecology and sequence stratigraphy of the Tunnel-Canal Dock, Belgium, *Geol. Mag.*, 146, 92–112, <https://doi.org/10.1017/S0016756808005438>, 2009.
- Downie, C., Hussain, M. A., and Williams, G. L.: Dinoflagellate cyst and acritarch associations in the Pa-

- leogene of southeast England, *Geosci. Man*, 3, 29–35, <https://doi.org/10.1080/00721395.1971.9989706>, 1971.
- Dybkjær, K.: Dinocyst stratigraphy and palynofacies studies used for refining a sequence stratigraphic model – Uppermost Oligocene to lower Miocene, Jylland, Denmark, *Rev. Palaeobot. Palynol.*, 131, 201–249, <https://doi.org/10.1016/j.revpalbo.2004.03.006>, 2004.
- Dybkjær, K. and Rasmussen, E. S.: Organic-walled dinoflagellate cyst stratigraphy in an expanded Oligocene-Miocene boundary section in the eastern North Sea Basin (Frida-1 Well, Denmark) and correlation from basinal to marginal areas, *J. Micropalaeontol.*, 26, 1–17, <https://doi.org/10.1144/jm.26.1.1>, 2007.
- Dybkjær, K., Rasmussen, E. S., Śliwińska, K. K., Esbensen, K. H., and Mathiesen, A.: A palynofacies study of past fluvio-deltaic and shelf environments, the Oligocene-Miocene succession, North Sea Basin: A reference data set for similar Cenozoic systems, *Mar. Pet. Geol.*, 100, 111–147, <https://doi.org/10.1016/j.marpetgeo.2018.08.012>, 2019.
- Eaton, G. L.: Dinoflagellate cysts from the Bracklesham Beds (Eocene) of the Isle of Wight, southern England, *British Museum (Natural History) Geology, Bulletin*, 26, 227–332, 1976.
- Edwards, L. E.: Dinoflagellates, in: *Fossil prokaryotes and protists*, edited by: Lipps, J. H., Blackwell, Cambridge, 105–127, 1993.
- Egger, L. M., Śliwińska, K. K., van Peer, T. E., Liebrand, D., Lippert, P. C., Friedrich, O., Wilson, P. A., Norris, R. D., and Pross, J.: Magnetostratigraphically-calibrated dinoflagellate cyst bioevents for the uppermost Eocene to lowermost Miocene of the western North Atlantic (IODP Expedition 342, Paleogene Newfoundland sediment drifts), *Rev. Palaeobot. Palynol.*, 234, 159–185, <https://doi.org/10.1016/j.revpalbo.2016.08.002>, 2016.
- Eidvin, T., Riis, F., Rasmussen, E. S., and Rundberg, Y.: Investigation of Oligocene to Lower Pliocene deposits in the Nordic offshore area and onshore Denmark, *NPD Bull.*, 10, 1–62, 2013.
- Eidvin, T., Riis, F., and Rasmussen, E. S.: Oligocene to Lower Pliocene deposits of the Norwegian continental shelf, Norwegian Sea, Svalbard, Denmark and their relation to the uplift of Fennoscandia: A synthesis, *Mar. Pet. Geol.*, 56, 184–221, <https://doi.org/10.1016/j.marpetgeo.2014.04.006>, 2014.
- Eldrett, J. S., Harding, I. C., Firth, J. V., and Roberts, A. P.: Magnetostratigraphic calibration of Eocene-Oligocene dinoflagellate cyst biostratigraphy from the Norwegian-Greenland Sea, *Mar. Geol.*, 204, 91–127, [https://doi.org/10.1016/S0025-3227\(03\)00357-8](https://doi.org/10.1016/S0025-3227(03)00357-8), 2004.
- Eldrett, J. S., Harding, I. C., Wilson, P. A., Butler, E., and Roberts, A. P.: Continental ice in Greenland during the Eocene and Oligocene, *Nature*, 446, 176–179, <https://doi.org/10.1038/nature05591>, 2007.
- Eshet, Y., Almogi-Labin, A., and Bein, A.: Dinoflagellate cysts, paleoproductivity and upwelling systems: A Late Cretaceous example from Israel, *Mar. Micropaleontol.*, 23, 231–240, [https://doi.org/10.1016/0377-8398\(94\)90014-0](https://doi.org/10.1016/0377-8398(94)90014-0), 1994.
- Fensome, R. A., Guerstein, G. R., and Williams, G. L.: New insights on the Paleogene dinoflagellate cyst genera *Enneadocysta* and *Licracysta* gen. nov. based on material from offshore eastern Canada and southern Argentina, *Micropaleontology*, 52, 385–410, <https://doi.org/10.2113/gsmicropal.52.5.385>, 2006.
- Fyfe, J. A., Gregersen, U., Jord, H., Rundberg, Y., Evans, D., Stewart, D., Hovland, M., and Andersen, P.: Oligocene to Holocene, in: *The Millennium Atlas: petroleum geology of the central and northern North Sea*, edited by: Evans, D., Graham, C., Armour, A., and Bathurst, P., The Geological Society of London, London, 279–287, 2003.
- Galeotti, S., DeConto, R., Naish, T., Stocchi, P., Florindo, F., Pagani, M., Barrett, P., Bohaty, S. M., Lanci, L., Pollard, D., Sandroni, S., Talarico, F. M., and Zachos, J. C.: Antarctic Ice Sheet variability across the Eocene-Oligocene boundary climate transition, *Science*, 352, 76–80, <https://doi.org/10.1126/science.aab0669>, 2016.
- Gedl, P.: Dinoflagellate cyst record of the Eocene-Oligocene boundary succession in flysch deposits at Leluchów, Carpathian Mountains, Poland, *Geol. Soc. London, Spec. Publ.*, 230, 257–273, <https://doi.org/10.1144/GSL.SP.2004.230.01.13>, 2004.
- Head, M. J.: Morphology and Palaeoenvironmental Significance of the Cenozoic Dinoflagellate Genera *Tectatodinium* and *Habibacysta*, *Micropaleontology*, 40, 289–321, <https://doi.org/10.2307/1485937>, 1994.
- Head, M. J. and Norris, G.: Palynology and dinocyst stratigraphy of the Eocene and Oligocene in ODP leg 105, hole 647A, Labrador Sea, Ocean Drill. Program. Proc. Sci. Res., 105, 515–550, 1989.
- Heilmann-Clausen, C. and Van Simaey, S.: Dinoflagellate cysts from the Middle Eocene to lowermost Oligocene succession in the Kysing research borehole, central Danish basin, *Palynology*, 29, 143–204, <https://doi.org/10.1080/01916122.2005.9989606>, 2005.
- Huuse, M. and Clausen, O. R.: Morphology and origin of major Cenozoic sequence boundaries in the Eastern North Sea Basin: Top Eocene, near-top Oligocene and the mid-Miocene unconformity, *Basin Res.*, 13, 17–41, <https://doi.org/10.1046/j.1365-2117.2001.00123.x>, 2001.
- Jaramillo, C. A. and Oboh-Ikuenobe, F. E.: Sequence stratigraphic interpretations from palynofacies, dinocyst and lithological data of Upper Eocene–Lower Oligocene strata in southern Mississippi and Alabama, US Gulf Coast, *Palaeogeogr. Palaeoclimatol.*, 145, 259–302, [https://doi.org/10.1016/S0031-0182\(98\)00126-6](https://doi.org/10.1016/S0031-0182(98)00126-6), 1999.
- Jarsve, E. M., Eidvin, T., Nystuen, J. P., Faleide, J. I., Gabrielsen, R. H., and Thyberg, B. I.: The Oligocene succession in the eastern North Sea: Basin development and depositional systems, *Geol. Mag.*, 152, 668–693, <https://doi.org/10.1017/S0016756814000570>, 2015.
- King, C., Gale, A. S., and Barry, T. L.: A revised correlation of Tertiary rocks in the British Isles and adjacent areas of NW Europe, edited by: King, C., Gale, A. S., and Barry, T. L., Geological Society of London, 2016.
- Knox, R. W. O. B., Bosh, J. H. A., Rasmussen, E.S. Heilmann-Clausen, C., Hiss, M., Kasiński, J., King, C., Köthe, A., Stodkowska, B. and Standke, G., and Vandenberghe, N.: Cenozoic, in: *Petroleum Geological Atlas of the Southern Permian Basin Area*, edited by: Doornbal, J. C. and Stevenson, A. G., EAGE Publication B.V., Houten, 211–223, 2010.
- Köthe, A.: Paleogene dinoflagellates from northwest Germany: biostratigraphy and palaeoenvironment, *Geol. Jahrbuch. R. A.*, 118, 1–111, 1990.
- Köthe, A.: Tertiary dinocyst zonation in northern Germany, *Rev. Paleobiol.*, 22, 895–923, 2003.
- Köthe, A. and Piesker, B.: Stratigraphic distribution of Paleogene and Miocene dinocysts in Germany, *Rev. Paleobiol.*, 26, 1–39, 2007.

- Lagrou, D., Vandenberghe, N., Van Simaey, S., and Hus, J.: Magnetostratigraphy and rock magnetism of the Boom Clay (Rupelian stratotype) in Belgium, *Geol. en Mijnbouw/Netherlands J. Geosci.*, 83, 209–225, <https://doi.org/10.1017/S001677460002028X>, 2004.
- Lavier, L. L., Steckler, M. S., and Brigaud, F.: Climatic and tectonic control on the Cenozoic evolution of the West African margin, *Mar. Geol.*, 178, 63–80, [https://doi.org/10.1016/S0025-3227\(01\)00175-X](https://doi.org/10.1016/S0025-3227(01)00175-X), 2001.
- Lund, J. J.: A Lower Oligocene Norwegian Sea Dinoflagellate Cyst Found in the North Sea and in the Rupelian Type Area in Belgium, in Northern European Cenozoic Stratigraphy, Proc. 8th Biann. Meet. RCNNS/RCNPS, 83–90, 2002.
- Marret, F. and Zonneveld, K. A. F.: Atlas of modern organic-walled dinoflagellate cyst distribution, *Rev. Palaeobot. Palynol.*, 125, 1–200, [https://doi.org/10.1016/S0034-6667\(02\)00229-4](https://doi.org/10.1016/S0034-6667(02)00229-4), 2003.
- Michelsen, O. and Danielsen, M.: Sequence and systems tract interpretation of the epicontinental Oligocene deposits in the Danish North Sea, *Geol. Siliciclastic Shelf Seas Geol. Soc. Spec. Publ.*, 117, 1–13, 1996.
- Michelsen, O., Danielsen, M., Heilmann-Clausen, C., Jordt, H., Laursen, G. V., and Thomsen, E.: Cenozoic sequence stratigraphy in the eastern North Sea, Final report of the CENOS-project, 1–51, 1992.
- Michelsen, O., Thomsen, E., Danielsen, M., Heilmann-Clausen, C., Jordt, H., and Laursen, G. V.: Cenozoic Sequence Stratigraphy In The Eastern North Sea, Mesozoic Cenozoic Seq. Stratigr. Eur. Basins, 60, 91–118, <https://doi.org/10.2110/pec.98.02.0091>, 1998.
- Miller, K. G., Wright, J. D., and Fairbanks, R. G.: Unlocking the Ice House: Oligocene-Miocene oxygen isotopes, eustasy, and margin erosion, *J. Geophys. Res.-Sol. Ea.*, 96, 6829–6848, <https://doi.org/10.1029/90JB02015>, 1991.
- Miller, K. G., Mountain, G. S., Browning, J. V., Kominz, M., Sugarman, P. J., Christie-Blick, N., Katz, M. E., and Wright, J. D.: Cenozoic global sea level, sequences, and the New Jersey transect: Results from coastal plain and continental slope drilling, *Rev. Geophys.*, 36, 569–601, <https://doi.org/10.1029/98RG01624>, 1998.
- NPD_report: NPD Paper No. 23 Interpreted lithology, available at: http://factpages.npd.no/pbl/NPD_papers/170_01_NPD_Paper_No.23_Lithology_Well_11_10_1.pdf, 1969a.
- NPD_report: Well completion report Syracuse 11/10-1X Production License, available at: http://factpages.npd.no/pbl/wellbore_documents/170_11_10_1_COMPLETION_REPORT.pdf, 1969b.
- Pälike, H., Norris, R. D., Herrle, J. O., Wilson, P. A., Coxall, H. K., Lear, C. H., Shackleton, N. J., Tripathi, A. K., and Wade, B. S.: The heartbeat of the Oligocene climate system, *Science*, 314, 1894–1898, <https://doi.org/10.1126/science.1133822>, 2006.
- Pekar, S. and Miller, K. G.: New Jersey Oligocene “Icehouse” sequences (ODP Leg 150X) correlated with global $\delta^{18}\text{O}$ and Exxon eustatic records, *Geology*, 24, 567–570, 1996.
- Pekar, S. F., Miller, K. G., and Kominz, M. A.: Reconstructing the stratal geometry of latest Eocene to Oligocene sequences in New Jersey: Resolving a patchwork distribution into a clear pattern of progradation, *Sediment. Geol.*, 134, 93–109, 2000.
- Pekar, S. F., Christie-Blick, N., Kominz, M. A., and Miller, K. G.: Calibration between eustatic estimates from backstripping and oxygen isotopic records for the Oligocene, *Geology*, 30, 903–906, 2002.
- Powell, A. J., Lewis, J., and Dodge, J. D.: The palynological expressions of post-Palaeogene upwelling: a review, *Geol. Soc. Lond. Sp. Publ.*, 64, 215–226, 1992.
- Pross, J.: Dinoflagellate cyst biogeography and biostratigraphy as a tool for palaeoceanographic reconstructions: An example from the Oligocene of western and northwestern Europe, *Neues Jahrb. Geol. P.-A.*, 219, 207–219, 2001a.
- Pross, J.: Paleo-oxygenation in tertiary epeiric seas: Evidence from dinoflagellate cysts, *Palaeogeogr. Palaeoclimatol.*, 166, 369–381, [https://doi.org/10.1016/S0031-0182\(00\)00219-4](https://doi.org/10.1016/S0031-0182(00)00219-4), 2001b.
- Pross, J. and Schmiedl, G.: Early Oligocene dinoflagellate cysts from the Upper Rhine Graben (SW Germany), *Mar. Micropaleontol.*, 45, 1–24, <https://doi.org/10.1594/PANGAEA.736658>, 2002.
- Pross, J., Houben, A. J. P., van Simaey, S., Williams, G. L., Kotthoff, U., Coccioni, R., Wilpshaar, M., and Brinkhuis, H.: Umbria-Marche revisited: A refined magnetostratigraphic calibration of dinoflagellate cyst events for the Oligocene of the Western Tethys, *Rev. Palaeobot. Palynol.*, 158, 213–235, <https://doi.org/10.1016/j.revpalbo.2009.09.002>, 2010.
- Rasmussen, E. S., Dybkjær, K., and Piasecki, S.: Lithostratigraphy of the Upper Oligocene – Miocene succession of Denmark, *Geological Survey of Denmark and Greenland Bulletin*, 22, 92 pp., 2010.
- Schiøler, P.: Dinoflagellate cysts and acritarchs from the Oligocene–Lower Miocene interval of the Alma-1X well, Danish North Sea, *J. Micropaleontol.*, 24, 1–37, <https://doi.org/10.1144/jm.24.1.1>, 2005.
- Schiøler, P., Andsbjerg, J., Clausen, O. R., Dam, G., Dybkjaer, K., Hamberg, L., Heilmann-Clausen, C., Johannessen, E. P., Kristensen, L. E., Prince, I., and Rasmussen, J. A.: Lithostratigraphy of the Palaeogene – Lower Neogene succession of the Danish North Sea, *Geol. Surv. Denmark Greenl. Bull.*, 12, 1–77, 2007.
- Śliwińska, K. K.: MSc thesis. North Sea Basin depositional history in relation to climatic trends during the Oligocene – elucidated with dinoflagellates, Department of Earth Sciences, Aarhus University, 74 pp., 2009.
- Śliwińska, K. K.: PhD. dissertation: The depositional history of the Oligocene in the North Sea Basin in relation to the climatic development, Department of Earth Sciences, Aarhus University, Aarhus, 90 pp., 2011.
- Śliwińska, K. K. and Heilmann-Clausen, C.: Early Oligocene cooling reflected by the dinoflagellate cyst *Svalbardella cooksoniae*, *Palaeogeogr. Palaeoclimatol.*, 305, 138–149, <https://doi.org/10.1016/j.palaeo.2011.02.027>, 2011.
- Śliwińska, K. K., Clausen, O. R., and Heilmann-Clausen, C.: A mid-Oligocene cooling (Oi-2b) reflected in the dinoflagellate record and in depositional sequence architecture. An integrated study from the eastern North Sea Basin, *Mar. Pet. Geol.*, 27, 1424–1430, <https://doi.org/10.1016/j.marpetgeo.2010.03.008>, 2010.
- Śliwińska, K. K., Abrahamsen, N., Beyer, C., Brünings-Hansen, T., Thomsen, E., Ulleberg, K., and Heilmann-Clausen, C.: Bio- and magnetostratigraphy of Rupelian-mid Chattian deposits from the Danish land area, *Rev. Palaeobot. Palynol.*, 172, 48–69, <https://doi.org/10.1016/j.revpalbo.2012.01.008>, 2012.

- Śliwińska, K. K., Heilmann-Clausen, C., and Thomsen, E.: Correlation Between the Type Chattian in NW Europe and the Rupelian–Chattian Candidate GSSP in Italy, in: STRATI 2013, Springer Geology, edited by: Rocha, R., Pais, J., Kullberg, J., and Finney, S., Springer, Cham, https://doi.org/10.1007/978-3-319-04364-7_57, 2014a.
- Śliwińska, K. K., Dybkjær, K., Schoon, P. L., Beyer, C., King, C., Schouten, S., and Nielsen, O. B.: Paleoclimatic and paleoenvironmental records of the Oligocene-Miocene transition, central Jylland, Denmark, *Mar. Geol.*, 350, 1–15, <https://doi.org/10.1016/j.margeo.2013.12.014>, 2014b.
- Śliwińska, K. K., Thomsen, E., Schouten, S., Schoon, P. L., and Heilmann-Clausen, C.: Climate- and gateway-driven cooling of Late eocene to earliest oligocene sea surface temperatures in the North sea Basin, *Sci. Rep.*, 9, 4458, <https://doi.org/10.1038/s41598-019-41013-7>, 2019.
- Sluijs, A., Pross, J., and Brinkhuis, H.: From greenhouse to icehouse; organic-walled dinoflagellate cysts as paleoenvironmental indicators in the Paleogene, *Earth-Sci. Rev.*, 68, 281–315, <https://doi.org/10.1016/j.earscirev.2004.06.001>, 2005.
- Snyder, S. W. and Waters, V. J.: Cenozoic planktonic foraminiferal biostratigraphy of the Goban Spur Region, Deep Sea Drilling Project Leg 80, in: Initial Reports of the Deep Sea Drilling Project, Vol. 80, edited by: Graciansky, P. C., Poag, C. W. et al., 80, 439–472, 1985.
- Sterrenburg, F. A. S., Hamilton, P., and Williams, D.: Universal coordinate method for locating light-microscope specimens, *Diatom Res.*, 27, 91–94, <https://doi.org/10.1080/0269249X.2012.688493>, 2012.
- Stover, L. E. and Hardenbol, J.: Dinoflagellates and depositional sequences in the Lower Oligocene (Rupelian) Boom Clay Formation, Belgium, *Bull. la Société belge géologie*, 102, 5–77, 1994.
- Sun, J., Ni, X., Bi, S., Wu, W., Ye, J., Meng, J., and Windley, B. F.: Synchronous turnover of flora, fauna, and climate at the Eocene-Oligocene Boundary in Asia, *Sci. Rep.*, 4, <https://doi.org/10.1038/srep07463>, 2014.
- Tripati, A. and Darby, D.: Evidence for ephemeral middle Eocene to early Oligocene Greenland glacial ice and pan-Arctic sea ice, *Nat. Commun.*, 9, <https://doi.org/10.1038/s41467-018-03180-5>, 2018.
- Vandenbergh, N., Hilgen, F. J., and Speijer, R. J.: The Geologic Time Scale 2012, edited by: Gradstein, F. M., Ogg, J. G., Schmitz, M., and Ogg, G., 855–921, 2012.
- Van Mourik, C. A. and Brinkhuis, H.: The Massignano Eocene-Oligocene golden spike section revisited, *Stratigraphy*, 2, 13–30, 2005.
- Van Simaey, S.: The Rupelian-Chattian boundary in the North Sea Basin and its calibration to the international time-scale, *Geol. en Mijnbouw/Netherlands, J. Geosci.*, 83, 241–248, <https://doi.org/10.1017/S0016774600020308>, 2004.
- Van Simaey, S. and Vandenbergh, N.: Rupelian, *Geol. Belg.*, 9, 95–101, 2006.
- Van Simaey, S., De Man, E., Vandenbergh, N., Brinkhuis, H., and Steurbaut, E.: Stratigraphic and palaeoenvironmental analysis of the Rupelian-Chattian transition in the type region: Evidence from dinoflagellate cysts, foraminifera and calcareous nannofossils, *Palaeogeogr. Palaeoclimatol.*, 208, 31–58, <https://doi.org/10.1016/j.palaeo.2004.02.029>, 2004.
- Van Simaey, S., Brinkhuis, H., Pross, J., Williams, G. L., and Zachos, J. C.: Arctic dinoflagellate migrations mark the strongest Oligocene glaciations, *Geology*, 33, 709–712, <https://doi.org/10.1130/G21634.1>, 2005a.
- Van Simaey, S., Munsterman, D., and Brinkhuis, H.: Oligocene dinoflagellate cyst biostratigraphy of the southern North Sea Basin, *Rev. Palaeobot. Palynol.*, 134, 105–128, <https://doi.org/10.1016/j.revpalbo.2004.12.003>, 2005b.
- Versteegh, G. J. M.: Recognition of cyclic and non-cyclic environmental changes in the Mediterranean Pliocene: A palynological approach, *Mar. Micropaleontol.*, 23, 147–183, [https://doi.org/10.1016/0377-8398\(94\)90005-1](https://doi.org/10.1016/0377-8398(94)90005-1), 1994.
- Wade, B. S. and Pälike, H.: Oligocene climate dynamics, *Paleoceanography*, 19, 1–16, <https://doi.org/10.1029/2004PA001042>, 2004.
- Wall, D., Dale, B., Lohmann, G. P., and Smith, W. K.: The environmental and climatic distribution of dinoflagellate cysts in modern marine sediments from regions in the North and South Atlantic Oceans and adjacent seas, *Mar. Micropaleontol.*, 2, 121–200, [https://doi.org/10.1016/0377-8398\(77\)90008-1](https://doi.org/10.1016/0377-8398(77)90008-1), 1977.
- Williams, G., Fensome, R., and MacRae, R.: The Lentins and Williams Index of Fossil Dinoflagellates 2017 Edition, *AASP Contrib. Ser.*, 48, 1–1097, 2017.
- Williams, G. L. and Downie, C.: Further dinoflagellate cysts from the London Clay, in: Studies on Mesozoic and Cainozoic dinoflagellate cysts, edited by: Davey, R. J., Downie, C., Sarjeant, W. A. S., and Williams, G. L., British Museum (Natural History) Geology, Bulletin, Supplement 3, 215–236, 1966.
- Williams, G. L. and Manum, S. B.: Oligocene – Early Miocene Dinocyst Stratigraphy of Hole 985a (Norwegian Sea), in: Proceedings of the Ocean Drilling Program, Scientific Results, Vol. 162, edited by: Raymo, M. E., Jansen, E., Blum, P., and Herbert, T. D., 99–109, 1999.
- Williams, G. L., Brinkhuis, H., Pearce, M. A., Fensome, R. A., and Weegink, J. W.: Southern Ocean and global dinoflagellate cyst events compared: Index events for the Late Cretaceous-Neogene, *Proc. Ocean Drill. Program, Sci. Results*, 189, 1–98, <https://doi.org/10.2973/odp.proc.sr.189.107.2004>, 2004.
- Zachos, J. C., Breza, J. R., and Wise, S. W.: Early Oligocene ice-sheet expansion on Antarctica: stable isotope and sedimentological evidence from Kerguelen Plateau, southern Indian Ocean, *Geology*, 20, 569–573, 1992.
- Zonneveld, K. A. F., Marret, F., Versteegh, G. J. M., Bogus, K., Bonnet, S., Bouimetarhan, I., Crouch, E., de Vernal, A., Elshanawany, R., Edwards, L., Esper, O., Forke, S., Grøsfjeld, K., Henry, M., Holzwarth, U., Kieft, J. F., Kim, S. Y., Ladouceur, S., Ledu, D., Chen, L., Limoges, A., Londeix, L., Lu, S. H., Mahmoud, M. S., Marino, G., Matsouka, K., Matthiessen, J., Mildenhall, D. C., Mudie, P., Neil, H. L., Pospelova, V., Qi, Y., Radi, T., Richerol, T., Rochon, A., Sangiorgi, F., Solignac, S., Turon, J. L., Verleye, T., Wang, Y., Wang, Z., and Young, M.: Atlas of modern dinoflagellate cyst distribution based on 2405 data points, *Rev. Palaeobot. Palynol.*, 191, 1–197, <https://doi.org/10.1016/j.revpalbo.2012.08.003>, 2013.